

# Dark Matter Direct Detection

- ❖ Kenny CY Ng
- ❖ [kcyng@cuhk.edu.hk](mailto:kcyng@cuhk.edu.hk)
- ❖ Sci Cen North Black 345
- ❖ CUHK
- ❖ Course webpage: <https://blackboard.cuhk.edu.hk>



# Does Dark Matter interact with Stuff?

- ❖ Direct Detection of Neutrinos?
- ❖ Neutrino-nucleon neutral current scattering is very small!
- ❖ However, these can be coherence

PHYSICAL REVIEW D

VOLUME 30, NUMBER 11

1 DECEMBER 1984

Principles and applications of a neutral-current detector  
for neutrino physics and astronomy

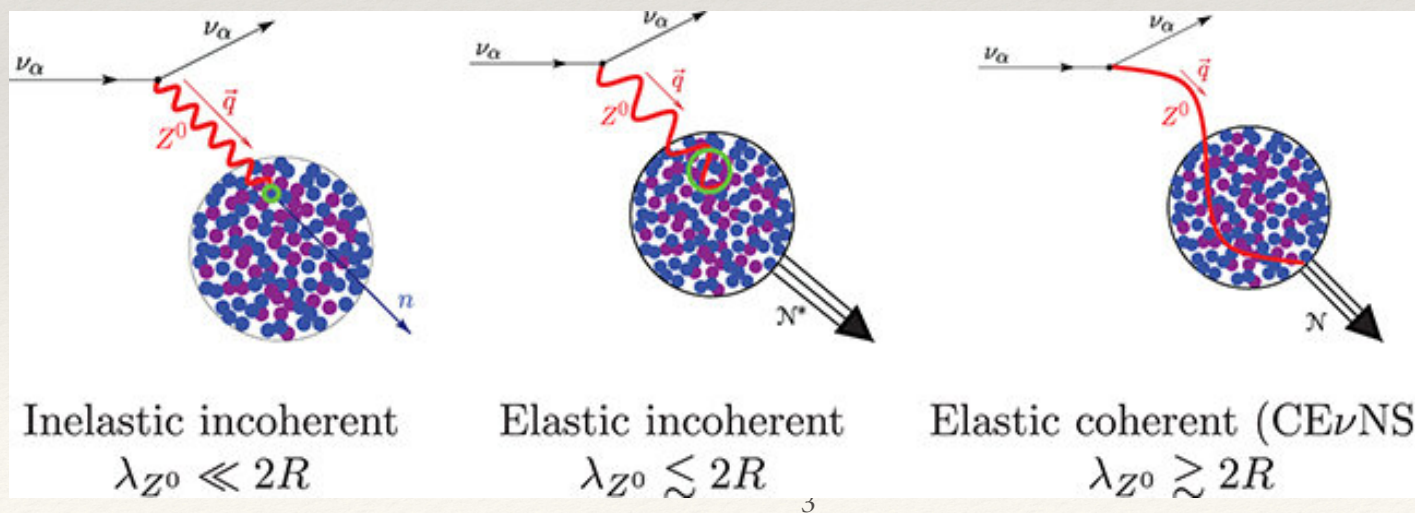
A. Drukier and L. Stodolsky  
*Max-Planck-Institut für Physik und Astrophysik, Werner-Heisenberg-Institut für Physik,  
Munich, Federal Republic of Germany*  
(Received 21 November 1983)

We study detection of MeV-range neutrinos through elastic scattering on nuclei and identification of the recoil energy. The very large value of the neutral-current cross section due to coherence indicates a detector would be relatively light and suggests the possibility of a true "neutrino observatory." The recoil energy which must be detected is very small ( $10-10^3$  eV), however. We examine a realization in terms of the superconducting-grain idea, which appears, in principle, to be feasible through extension and extrapolation of currently known techniques. Such a detector could permit determination of the neutrino energy spectrum and should be insensitive to neutrino oscillations since it detects all neutrino types. Various applications and tests are discussed, including spallation sources, reactors, supernovas, and solar and terrestrial neutrinos. A preliminary estimate of the most difficult backgrounds is attempted.

# Coherent Elastic Neutrino Nucleus Scattering

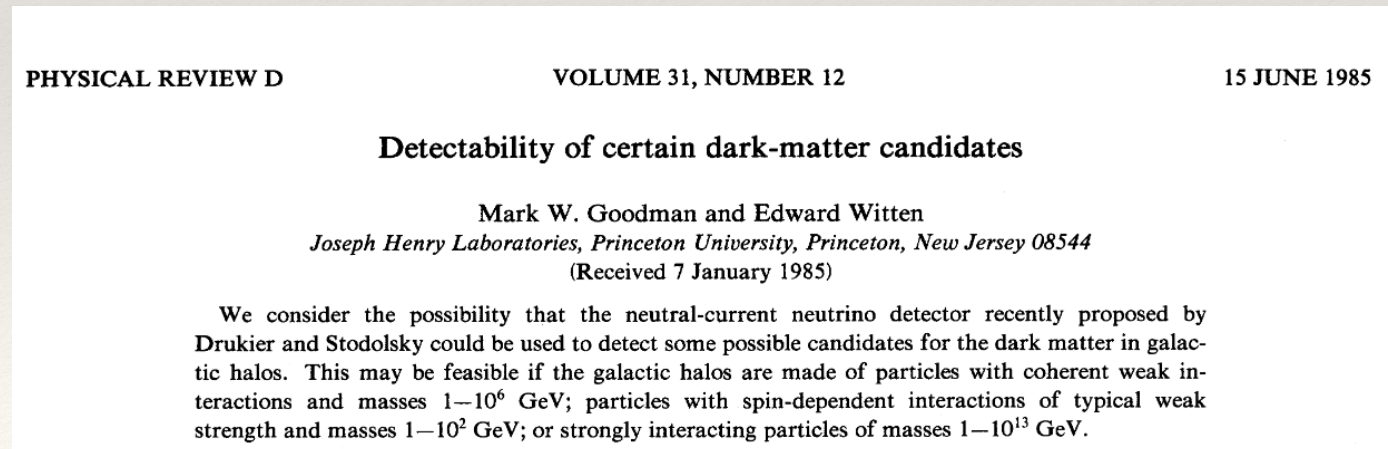
- ❖ CEvNS
- ❖ If the momentum transfer (energy) is small compared to the size (Length) of the nucleus
- ❖ The Neutrinos can see the whole nucleus
- ❖ The Quantum Mechanical Amplitude  $\langle \nu'N'|M|\nu N\rangle \propto N$  is proportional to the number of nucleons
- ❖ Then cross section (probability)  $\propto N^2$

- ❖ Incoherent scattering
  - ❖ Cross section  $\propto N$
  - ❖ If the nucleus is big, we can get large enhancements!



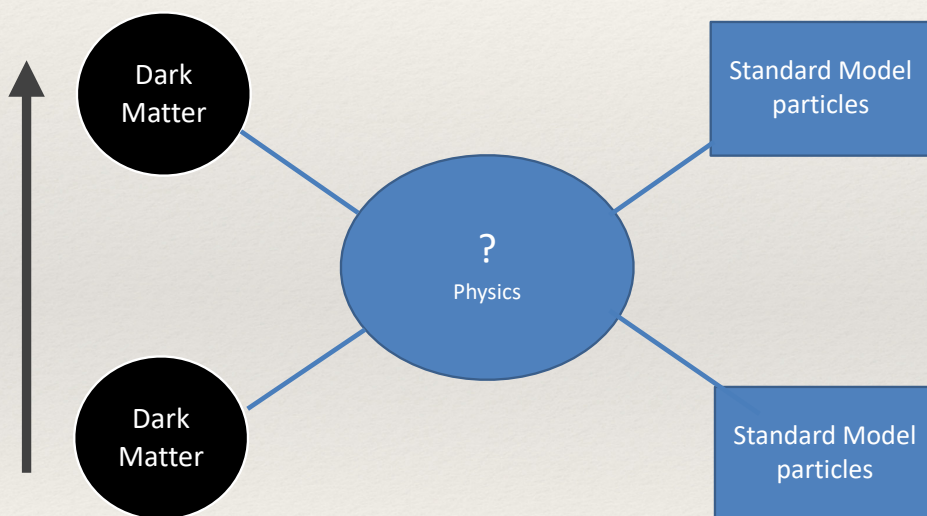
# Direct Detection of dark matter

- ❖ If dark matter has weak interaction, or weak-like interaction.
- ❖ It maybe possible to detect them through Elastic Scatterings!
- ❖ Possible candidates are like WIMPs.
  - ❖ Weakly Interacting Massive Particles

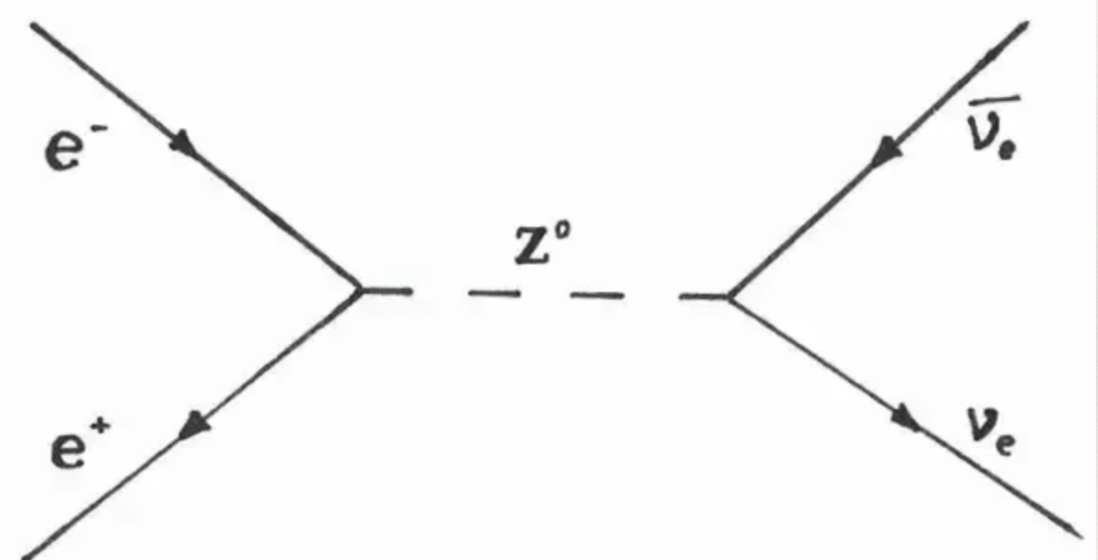


# Weakly Interacting Massive Particles (WIMPs)

## WIMPs



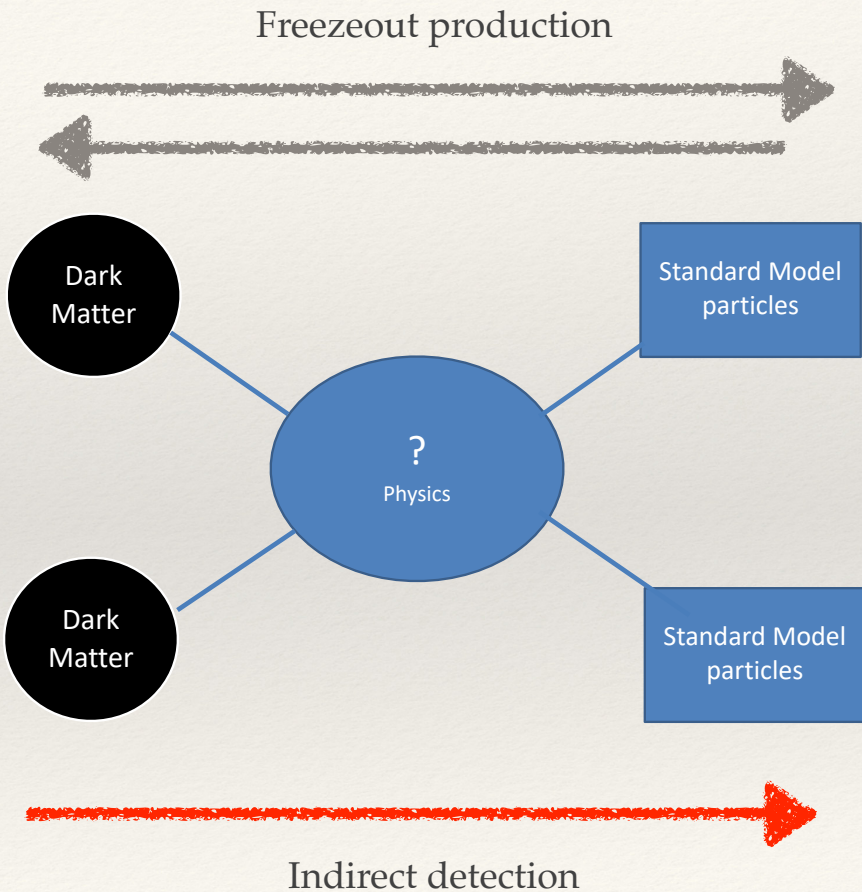
Direct Detection



Weak Interactions

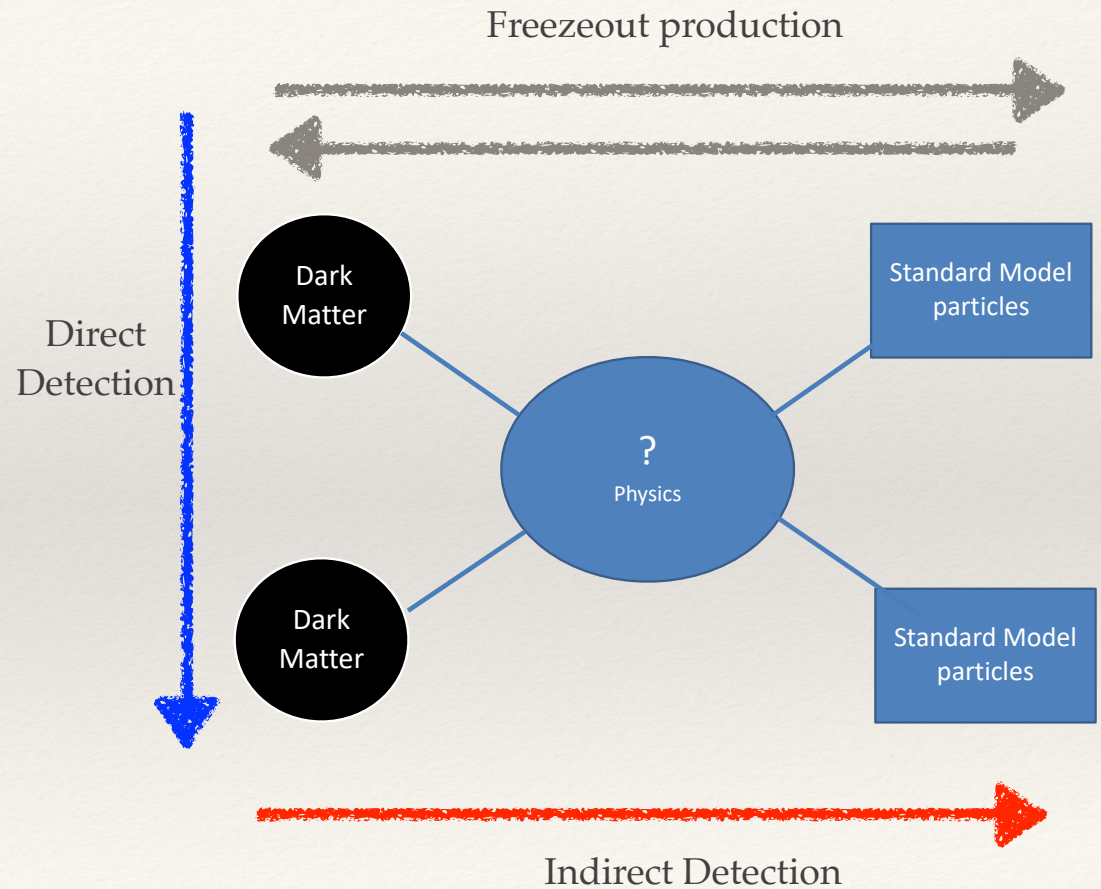
# Indirect Detection

- ❖ Freezeout mechanism predicts reactions
- ❖  $\chi\chi \rightarrow f\bar{f}$
- ❖ Where “f” can by any standard model particles
- ❖ The rate of this reaction needs to satisfy the Dark Matter abundance requirement.
- ❖ How to write down the annihilation rate?



# Dark Matter Direct Detection

- ❖ The WIMP hypothesis also predicts reactions like this
- ❖  $\chi + f \rightarrow f + \chi$
- ❖ Build a detector, hide underground and wait for interaction to happen.



---

# Dark Matter direct detection theory

---

- ❖ Build a detector on Earth and wait for dark matter to enter the detector and interact with
- ❖ Interaction rate
- ❖  $R \sim n_\chi n_t \sigma v \ dV$
- ❖ [Dark Matter number density] x [target number density] x [cross section] x [dark matter velocity] x [detector volume]

# Dark Matter velocity distribution

Simulated Milky Way analogues: implications for dark matter direct searches

Nassim Bozorgnia, Francesca Calore, Matthieu Schaller, Mark Lovell, Gianfranco Bertone, Carlos S. Frenk, Robert A. Crain, Julio F. Navarro, Joop Schaye and Tom Theuns

Published 11 May 2016 • © 2016 IOP Publishing Ltd and Sissa Medialab srl

[Journal of Cosmology and Astroparticle Physics, Volume 2016, May 2016](#)

Citation Nassim Bozorgnia et al JCAP05(2016)024

DOI 10.1088/1475-7516/2016/05/024

- ❖ We need to know the dark matter velocity at the solar system location
- ❖ [The Standard Halo Model]
  - ❖ Smooth dark matter halo , e.g., NFW
  - ❖ Maxwellian velocity distribution

$$f(|\mathbf{v}|) = v^2 \int d\Omega_{\mathbf{v}} \tilde{f}(\mathbf{v}), \quad (4.1)$$

such that  $\int d^3v \tilde{f}(\mathbf{v}) = 1$ . Here  $d\Omega_{\mathbf{v}}$  is an infinitesimal solid angle around the direction  $\mathbf{v}$ .

- Generalized Maxwellian distribution:

$$f(|\mathbf{v}|) \propto |\mathbf{v}|^2 \exp[-(|\mathbf{v}|/v_0)^{2\alpha}], \quad (4.2)$$

with free parameters  $v_0$  and  $\alpha$ . The case of a standard Maxwellian distribution is represented by  $\alpha = 1$ . We also test the goodness of fit for a standard Maxwellian to the simulated velocity modulus distributions (see [tables 2 and 3](#) in appendix C).

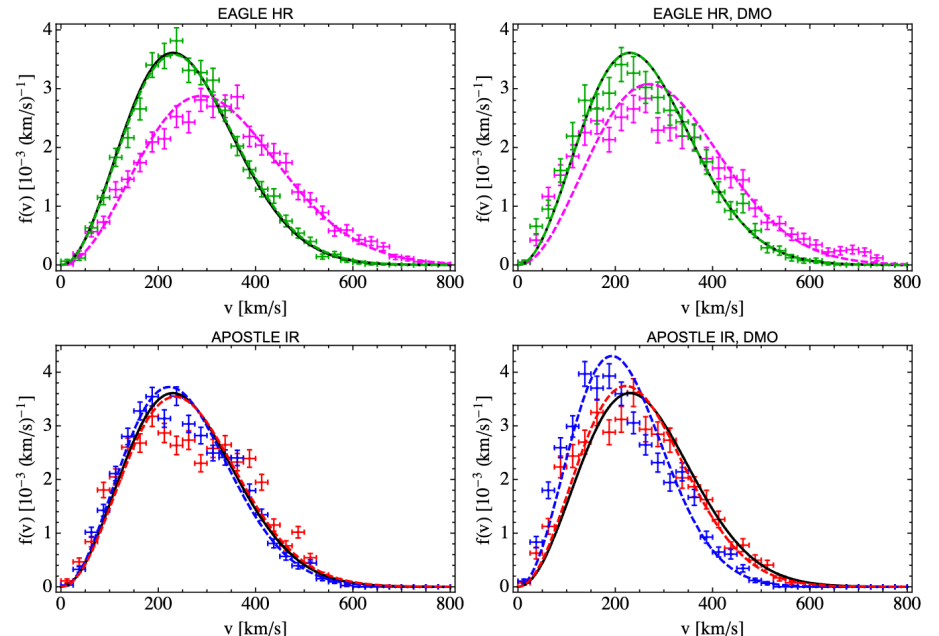


**Figure 2.** DM velocity modulus distributions in the Galactic rest frame (coloured data points with  $1\sigma$  error bars) for two haloes in the EAGLE HR simulation which satisfy our selection criteria and have the speed distributions closest to (halo E12, shown in green) and farthest from (halo E3, shown in magenta) the SHM Maxwellian (top left), and two haloes in the APOSTLE IR simulation satisfying our selection criteria (bottom left). The right panels show the velocity modulus distributions for the same haloes shown in the left panels but in a DMO simulation. The black solid line shows the SHM Maxwellian speed distribution (with peak speed of 230 km/s), and the coloured dashed lines show the best fit Maxwellian distribution for each halo (with matching colours).

# Dark Matter direct detection theory

- ❖ Build a detector on Earth and wait for dark matter to enter the detector and interact with
- ❖ Interaction rate
- ❖  $R \sim n_\chi n_t \sigma v \ dV$
- ❖ [Dark Matter number density]  $\times$  [target number density]  $\times$  [cross section]  $\times$  [dark matter velocity]  $\times$  [detector volume]
- ❖ Including velocity distribution
- ❖  $\longrightarrow R \sim n_\chi n_t \sigma(vf) dv dV$
- ❖ So far we only have discussed the rate of interaction
- ❖ To see the interaction, we need to specify what happens after interaction.
- ❖ The simplest interaction is “Elastic Interaction”, so a nuclei is recoiled after interaction.
- ❖ The recoiled energy  $E_{nr}$  is then of concern. A detector usually has some energy threshold, that it can only see events above the threshold

# Dark Matter direct detection theory

- ❖  $R \sim n_\chi n_t \sigma(vf) dv dV$
  - ❖ The differential interaction rate
  - ❖  $\frac{dR}{dE_{nr}} = n_\chi (\int n_t dV) \frac{d\sigma}{dE_{nr}} (vf dv)$
- The expected scattering rate is given by
- $$\begin{aligned} \frac{dR}{dE_{nr}} &= \frac{\rho_0 M}{m_N m_\chi} \int_{v_{\min}}^{\infty} v f(v) \frac{d\sigma}{dE_{nr}} dv \\ &\propto \exp\left(-\frac{E_{nr}}{E_0} \frac{4m_\chi m_N}{(m_\chi + m_N)^2}\right) F^2(E_{nr}), \end{aligned}$$
- ❖ So far we only have discussed the rate of interaction
  - ❖ To see the interaction, we need to specify what happens after interaction.
  - ❖ The simplest interaction is “Elastic Interaction”, so a nuclei is recoiled after interaction.
  - ❖ The recoiled energy  $E_{nr}$  is then of concern. A detector usually has some energy threshold, that it can only see events above the threshold

- ❖  $v_{\min}$  is the minimum DM velocity to trigger the detector

# SI or SD

- ❖ The precise type of interaction again depends on the underlying dark matter theory
- ❖ In the non-relativistic limit, there are two types:
  - ❖ **Spin independent**
    - ❖ Gets the  $A^2$  coherent enhancement term
  - ❖ **Spin dependent**
    - ❖ Need the nucleus to have non-zero spin
    - ❖ Does not get  $A^2$  enhancement

The *spin-independent* (SI) cross section is given by

$$\sigma_{SI} = \sigma_n \frac{\mu^2}{\mu_n^2} \frac{(f_p Z + f_n(A - Z))^2}{f_n^2} = \sigma_n \frac{\mu^2}{\mu_n^2} A^2.$$

- ❖ Here  $\sigma_n$  is the dark matter nucleon cross section
- ❖  $\sigma_{SI}$  is the dark matter “nucleus” cross section

TABLE IV. The kinematic suppression of the spin-independent and spin-dependent scattering cross sections for all possible interaction structures. F1–F10 correspond to fermionic dark matter (with F5, F7, F9 and F10 absent for Majorana fermions), S1–S4 correspond to real or complex scalar dark matter, V1–V10 to real or complex vector dark matter. Each suppression is labeled to indicate if it arises from the SM or dark matter (DM) bilinear. If a cross section contains several terms with different kinematic suppressions, each is listed on a separate line. We also list if  $s$ -wave annihilation is permitted and unsuppressed, if it is chirality suppressed by a factor  $\propto m_f^2/m_X^2$ , or if it is not permitted at all; although the interactions are expressed in terms of quark fields  $q$ , by a slight abuse of notation we allow for annihilation to any pair of SM fermions  $\bar{f}f$ , each of mass  $m_f$ .

Name	Interaction structure	$\sigma_{\text{SI}}$ suppression	$\sigma_{\text{SD}}$ suppression	$s$ -wave?
F1	$\bar{X}X\bar{q}q$	1	$q^2 v^{\perp 2}$ (SM)	No
F2	$\bar{X}\gamma^5 X\bar{q}q$	$q^2$ (DM)	$q^2 v^{\perp 2}$ (SM); $q^2$ (DM)	Yes
F3	$\bar{X}X\bar{q}\gamma^5 q$	0	$q^2$ (SM)	No
F4	$\bar{X}\gamma^5 X\bar{q}\gamma^5 q$	0	$q^2$ (SM); $q^2$ (DM)	Yes
F5	$\bar{X}\gamma^\mu X\bar{q}\gamma_\mu q$ (vanishes for Majorana $X$ )	1	$q^2 v^{\perp 2}$ (SM)	Yes
F6	$\bar{X}\gamma^\mu \gamma^5 X\bar{q}\gamma_\mu q$	$v^{\perp 2}$ (SM or DM)	$q^2$ (SM)	No
F7	$\bar{X}\gamma^\mu X\bar{q}\gamma_\mu \gamma^5 q$ (vanishes for Majorana $X$ )	$q^2 v^{\perp 2}$ (SM); $q^2$ (DM)	$v^{\perp 2}$ (SM)	Yes
F8	$\bar{X}\gamma^\mu \gamma^5 X\bar{q}\gamma_\mu \gamma^5 q$	$q^2 v^{\perp 2}$ (SM)	1	$\propto m_f^2/m_X^2$
F9	$\bar{X}\sigma^{\mu\nu} X\bar{q}\sigma_{\mu\nu} q$ (vanishes for Majorana $X$ )	$q^2$ (SM); $q^2$ or $v^{\perp 2}$ (DM)	1	Yes
F10	$\bar{X}\sigma^{\mu\nu} \gamma^5 X\bar{q}\sigma_{\mu\nu} q$ (vanishes for Majorana $X$ )	$q^2$ (SM)	$v^{\perp 2}$ (SM)	Yes
S1	$\phi^\dagger \phi \bar{q}q$ or $\phi^2 \bar{q}q$	1	$q^2 v^{\perp 2}$ (SM)	Yes
S2	$\phi^\dagger \phi \bar{q}\gamma^5 q$ or $\phi^2 \bar{q}\gamma^5 q$	0	$q^2$ (SM)	Yes
S3	$\phi^\dagger \partial_\mu \phi \bar{q}\gamma^\mu q$	1	$q^2 v^{\perp 2}$ (SM)	No
S4	$\phi^\dagger \partial_\mu \phi \bar{q}\gamma^\mu \gamma^5 q$	0	$v^{\perp 2}$ (SM or DM)	No
V1	$B_\mu^\dagger B^\mu \bar{q}q$ or $B_\mu B^\mu \bar{q}q$	1	$q^2 v^{\perp 2}$ (SM)	Yes
V2	$B_\mu^\dagger B^\mu \bar{q}\gamma^5 q$ or $B_\mu B^\mu \bar{q}\gamma^5 q$	0	$q^2$ (SM)	Yes
V3	$B_\nu^\dagger \partial_\mu B^\nu \bar{q}\gamma^\mu q$	1	$q^2 v^{\perp 2}$ (SM)	No
V4	$B_\nu^\dagger \partial_\mu B^\nu \bar{q}\gamma^\mu \gamma^5 q$	0	$v^{\perp 2}$ (SM or DM)	No
V5	$(B_\mu^\dagger B_\nu - B_\nu^\dagger B_\mu) \bar{q}\sigma^{\mu\nu} q$	$q^2 v^{\perp 2}$ (SM)	1	Yes
V6	$(B_\mu^\dagger B_\nu - B_\nu^\dagger B_\mu) \bar{q}\sigma^{\mu\nu} \gamma^5 q$	$q^2$ (SM)	$v^{\perp 2}$ (SM)	Yes
V7	$B_\nu^\dagger \partial^\nu B_\mu \bar{q}\gamma^\mu q$ or $B_\nu \partial^\nu B_\mu \bar{q}\gamma^\mu q$	$v^{\perp 2}$ (SM); $q^2$ (DM)	$q^2$ (SM); $q^2$ (DM)	No
V8	$B_\nu^\dagger \partial^\nu B_\mu \bar{q}\gamma^\mu \gamma^5 q$ or $B_\nu \partial^\nu B_\mu \bar{q}\gamma^\mu \gamma^5 q$	$q^2 v^{\perp 2}$ (SM); $q^2$ (DM)	$q^2$ (DM)	$\propto m_f^2/m_X^2$
V9	$\epsilon^{\mu\nu\rho\sigma} B_\nu^\dagger \partial_\rho B_\sigma \bar{q}\gamma_\mu q$ or $\epsilon^{\mu\nu\rho\sigma} B_\nu \partial_\rho B_\sigma \bar{q}\gamma_\mu q$	$v^{\perp 2}$ (DM or SM)	$q^2$ (SM)	No
V10	$\epsilon^{\mu\nu\rho\sigma} B_\nu^\dagger \partial_\rho B_\sigma \bar{q}\gamma_\mu \gamma^5 q$ or $\epsilon^{\mu\nu\rho\sigma} B_\nu \partial_\rho B_\sigma \bar{q}\gamma_\mu \gamma^5 q$	$q^2 v^{\perp 2}$ (SM)	1	No

PHYSICAL REVIEW D 88, 014035 (2013)

## Matrix element analyses of dark matter scattering and annihilation

Jason Kumar<sup>1</sup> and Danny Marfatia<sup>2</sup>

<sup>1</sup>Department of Physics and Astronomy, University of Hawaii, Honolulu, Hawaii 96822, USA  
<sup>2</sup>Department of Physics and Astronomy, University of Kansas, Lawrence, Kansas 66045, USA

(Received 12 May 2013; published 23 July 2013)

We provide a compendium of results at the level of matrix elements for a systematic study of dark matter scattering and annihilation. We identify interactions that yield spin-dependent and spin-independent scattering and specify whether the interactions are velocity and/or momentum suppressed. We identify the interactions that lead to  $s$ -wave or  $p$ -wave annihilation, and those that are chirality suppressed. We also list the interaction structures that can interfere in scattering and annihilation processes. Using these results, we point out situations in which deviations from the standard lore are obtained.

DOI: 10.1103/PhysRevD.88.014035

PACS numbers: 14.65.Jk, 13.85.Rm, 95.35.+d

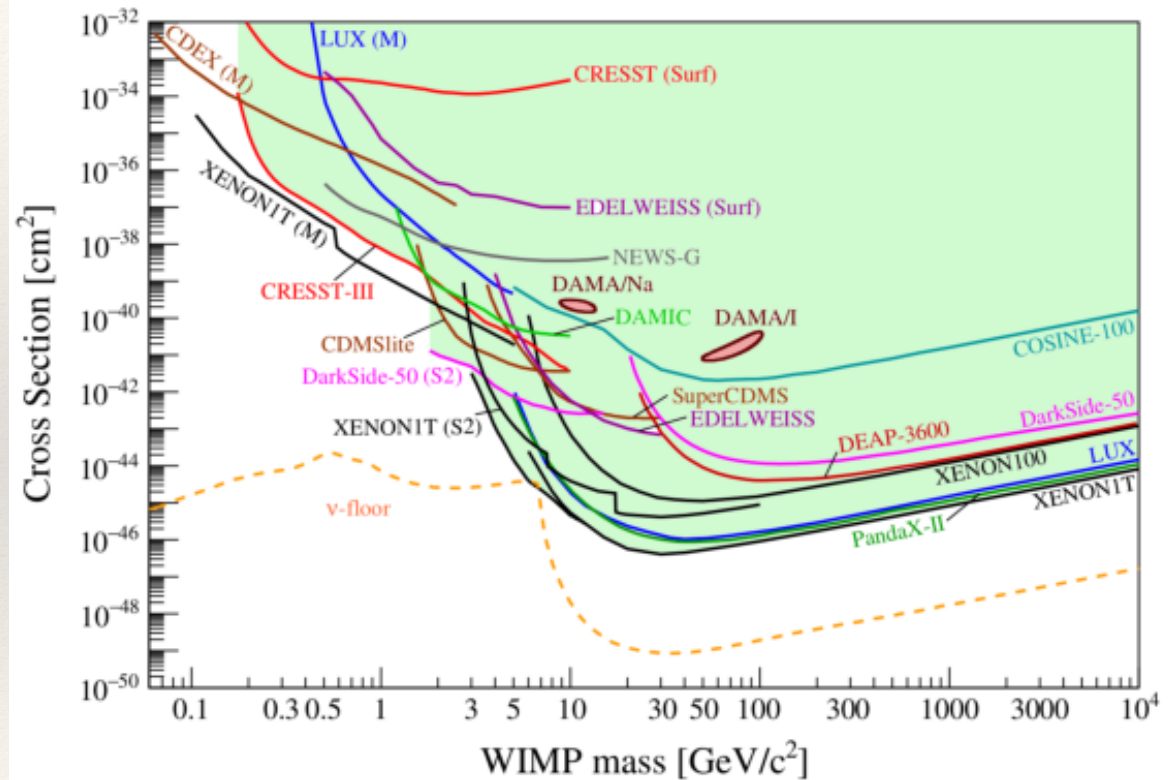


# Dark Matter direct detection

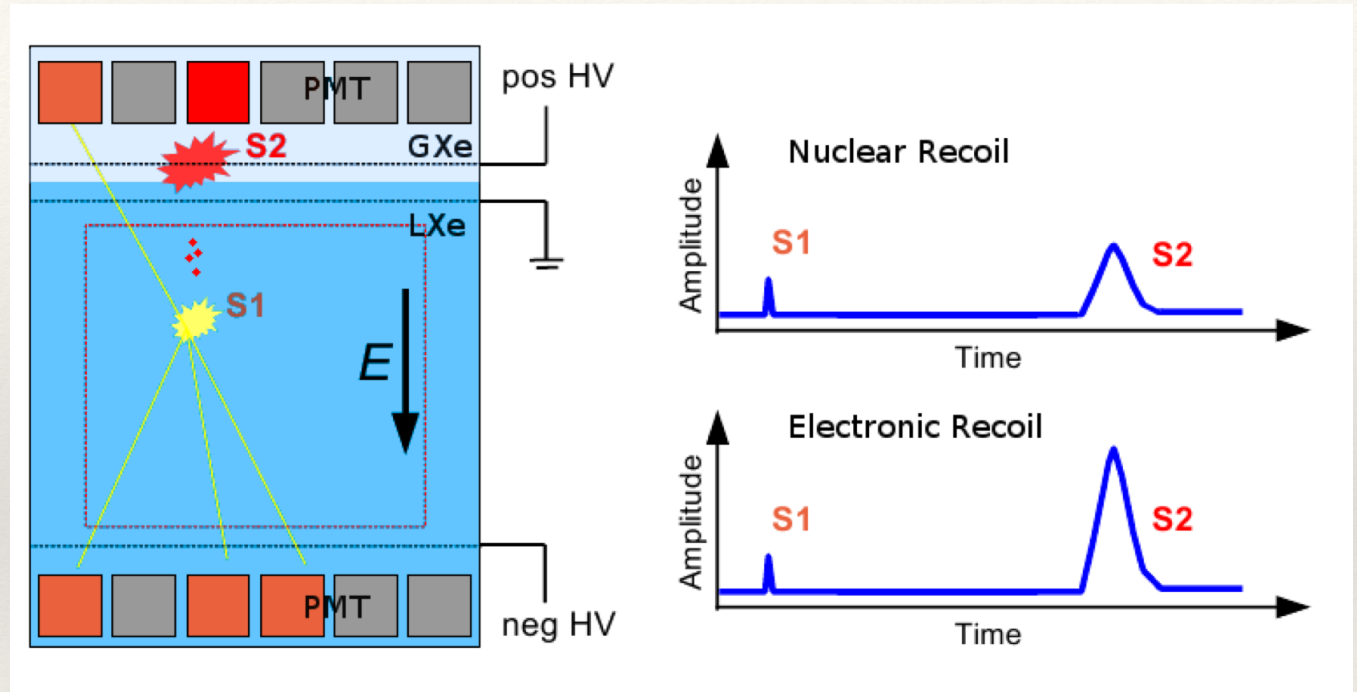
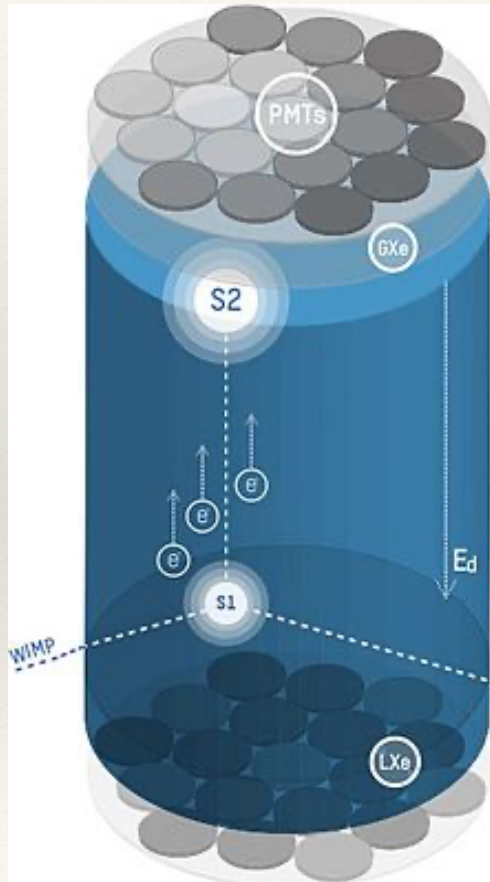
- ❖ We can estimate the recoil energy
- ❖ The incoming dark matter momentum is about  $m_\chi v$
- ❖ If transferred to the nuclei
- ❖ The nuclei will have kinetic energy about
- ❖ 
$$E_r \sim \frac{(m_\chi v)^2}{m_N}$$
- ❖ If  $M_N \sim 100 \text{ GeV}$ ,  $m_\chi \sim 1 \text{ GeV}$ ,  $v \sim 10^{-3}c$
- ❖ Then  $E_r \sim 10 \text{ eV}$
- ❖ Extremely sensitive detectors!

# Dark Matter direct detection

- ❖ General features
- ❖ Peak sensitivity
- ❖ When  $m_\chi \sim m_N$
- ❖ When  $m_\chi > m_N$ 
  - ❖ Event rate drops due to  $\rho/m_\chi$
- ❖ When  $m_\chi < m_N$ 
  - ❖ Detector threshold rapidly limits sensitivity
  - ❖  $\Leftrightarrow$  hard for dark matter to produce a recoil to trigger the detector
  - ❖ Relies on the high velocity tail of the dark matter velocity distribution
    - ❖  $\sim$  exponential function



# E.g., XENON



- ❖ Dual phase detector
  - ❖ S1: Recoil produces scintillation light
  - ❖ S2: Electric field push the ionisation electrons to the top, Gas phase, produce another scintillation signal

## Astrophysics &gt; Cosmology and Nongalactic Astrophysics

*[Submitted on 31 May 2018 (v1), last revised 13 Sep 2018 (this version, v2)]*

# Dark Matter Search Results from a One Tonne×Year Exposure of XENON1T

E. Aprile, J. Aalbers, F. Agostini, M. Alfonsi, L. Althueser, F. D. Amaro, M. Anthony, F. Arneodo, L. Baudis, B. Bauermeister, M. L. Benabderahmane, T. Berger, P. A. Breur, A. Brown, A. Brown, E. Brown, S. Bruenner, G. Bruno, R. Budnik, C. Capelli, J. M. R. Cardoso, D. Cichon, D. Coderre, A. P. Colijn, J. Conrad, J. P. Cussonneau, M. P. Decowski, P. de Perio, P. Di Gangi, A. Di Giovanni, S. Diglio, A. Elykov, G. Eurin, J. Fei, A. D. Ferella, A. Fieguth, W. Fulgione, A. Gallo Rosso, M. Galloway, F. Gao, M. Garbini, C. Geis, L. Grandi, Z. Greene, H. Qiu, C. Hasterok, E. Hogenbirk, J. Howlett, R. Itay, F. Joerg, B. Kaminsky, S. Kazama, A. Kish, G. Koltman, H. Landsman, R. F. Lang, L. Levinson, Q. Lin, S. Lindemann, M. Lindner, F. Lombardi, J. A. M. Lopes, J. Mahlstedt, A. Manfredini, T. Marrodán Undagoitia, J. Masbou, D. Masson, M. Messina, K. Micheneau, K. Miller, A. Molinario, K. Morå, M. Murra, J. Naganoma, K. Ni, U. Oberlack, B. Pelssers, F. Piastra, J. Pienaar, V. Pizzella, G. Plante, R. Podviianiuk, N. Priel, D. Ramírez García, L. Rauch, S. Reichard, C. Reuter, B. Riedel, A. Rizzo, A. Rocchetti, N. Rupp, J. M. F. dos Santos, G. Sartorelli, M. Scheibelhut, S. Schindler, J. Schreiner, D. Schulte, M. Schumann, L. Scotto Lavina, M. Selvi et al. (20 additional authors not shown)

We report on a search for Weakly Interacting Massive Particles (WIMPs) using 278.8 days of data collected with the XENON1T experiment at LNGS. XENON1T utilizes a liquid xenon time projection chamber with a fiducial mass of  $(1.30 \pm 0.01)$  t, resulting in a  $1.0 \text{ t} \times \text{yr}$  exposure. The energy region of interest,  $[1.4, 10.6] \text{ keV}_{\text{ee}}$  ( $[4.9, 40.9] \text{ keV}_{\text{nr}}$ ), exhibits an ultra-low electron recoil background rate of  $(82^{+5}_{-3} \text{ (sys)} \pm 3 \text{ (stat)}) \text{ events}/(\text{t} \times \text{yr} \times \text{keV}_{\text{ee}})$ . No significant excess over background is found and a profile likelihood analysis parameterized in spatial and energy dimensions excludes new parameter space for the WIMP-nucleon spin-independent elastic scatter cross-section for WIMP masses above  $6 \text{ GeV}/c^2$ , with a minimum of  $4.1 \times 10^{-47} \text{ cm}^2$  at  $30 \text{ GeV}/c^2$  and 90% confidence level.

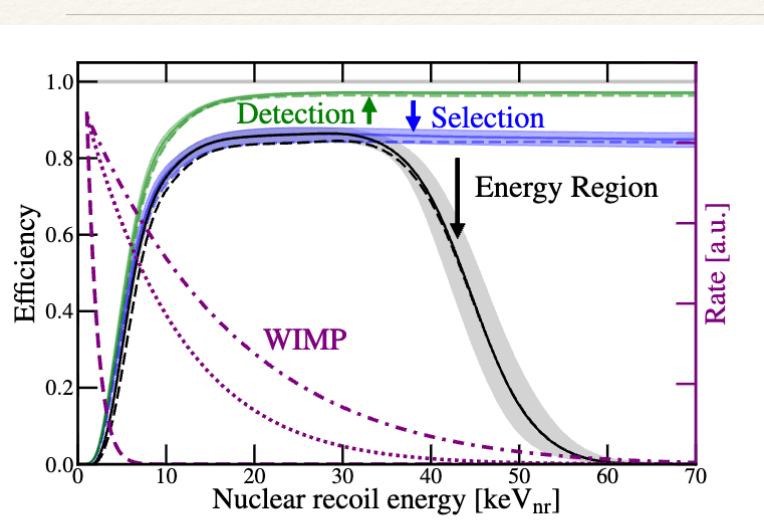


FIG. 1: Best-fit total efficiencies (black), including the energy ROI selection, for SR0 (dashed) and SR1 (solid) as a function of true NR energy ( $\text{keV}_{\text{nr}}$ ). The efficiency of S1 detection (green) and that of S1 detection and selection (blue) are shown. The shaded bands show the 68% credible regions for SR1. The expected spectral shapes (purple) of  $10 \text{ GeV}/c^2$  (dashed),  $50 \text{ GeV}/c^2$  (dotted), and  $200 \text{ GeV}/c^2$  (dashed dotted) WIMPs are overlaid for reference.

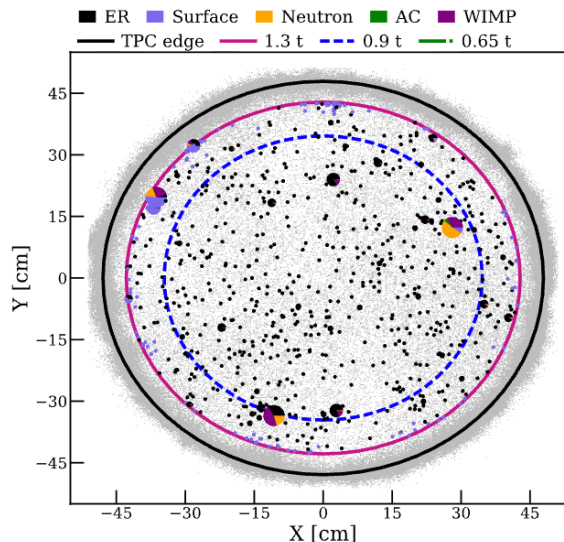


FIG. 2: Spatial distributions of DM search data. Events that pass all selection criteria and are within the fiducial mass are drawn as pie charts representing the relative probabilities of the background and signal components for each event under the best-fit model (assuming a  $200 \text{ GeV}/c^2$  WIMP and resulting best-fit  $\sigma_{SI} = 4.7 \times 10^{-47} \text{ cm}^2$ ) with color code given in the legend. Small charts (mainly single-colored) correspond to unambiguously background-like events, while events with larger WIMP probability are drawn progressively larger. Gray points are events reconstructed outside the fiducial mass. The TPC boundary (black line),  $1.3 \text{ t}$  fiducial mass (magenta), maximum radius of the reference  $0.9 \text{ t}$  mass (blue dashed), and  $0.65 \text{ t}$  core mass (green dashed) are shown. Yellow shaded regions display the  $1\sigma$  (dark) and  $2\sigma$  (light) probability density percentiles of the radiogenic neutron background component for SR1.

# S1/S2 ratio to eliminate electron like events

## ❖ Data

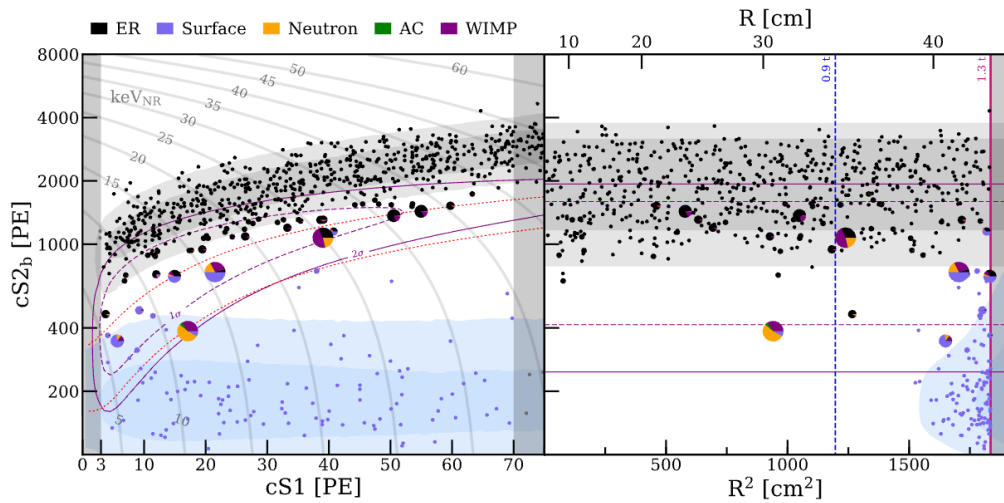


FIG. 3: DM search data in the 1.3 t fiducial mass distributed in (cS1, cS2<sub>b</sub>) (left) and ( $R^2$ , cS2<sub>b</sub>) (right) parameter spaces with the same marker descriptions as in Fig. 2. Shaded regions are similar to Fig. 2, showing the projections in each space of the surface (blue) and ER (gray) background components for SR1. The 1 $\sigma$  (purple dashed) and 2 $\sigma$  (purple solid) percentiles of a 200 GeV/c<sup>2</sup> WIMP signal are overlaid for reference. Vertical shaded regions are outside the ROI. The NR signal reference region (left, between the two red dotted lines) and the maximum radii (right) of the 0.9 t (blue dashed) and 1.3 t (magenta solid) masses are shown. Gray lines show iso-energy contours in NR energy.

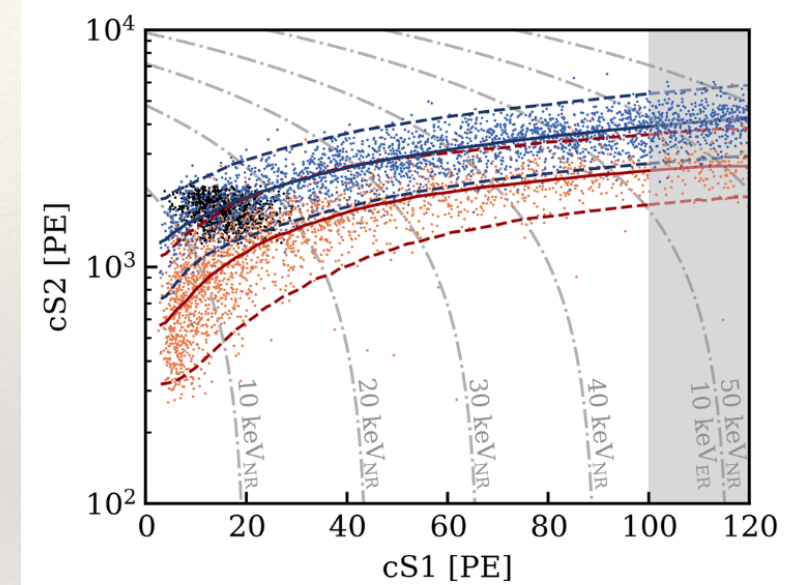


FIG. 1. NR and ER calibration data from <sup>241</sup>AmBe (orange), <sup>222</sup>Rn (blue), and <sup>37</sup>Ar (black). The median and the  $\pm 2\sigma$  contours of the NR and ER model are shown in blue and red, respectively. The gray dash-dotted contour lines show the reconstructed NR energy (keV<sub>NR</sub>). Only not shaded events up to a cS1 of 100 PE are considered in the response model fits.

## ❖ Calibration using known sources

# S1/S2 ratio to eliminate electron like events

- ❖ Non detection
  - ❖ Sets a limit on the dark matter nucleon interaction cross section

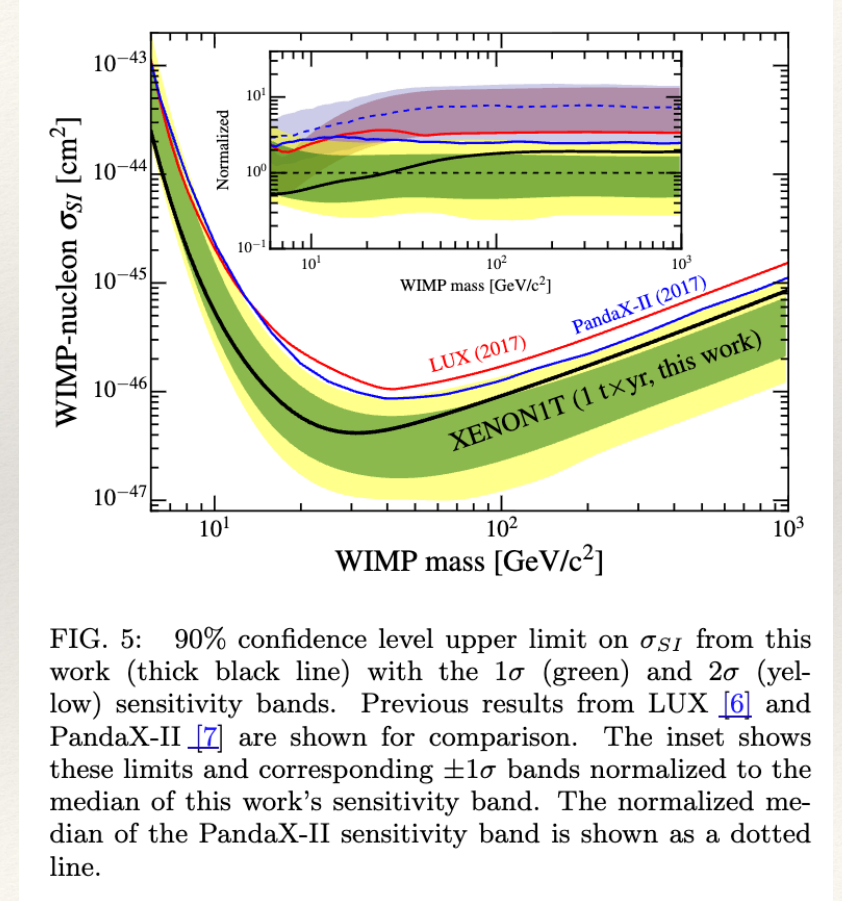
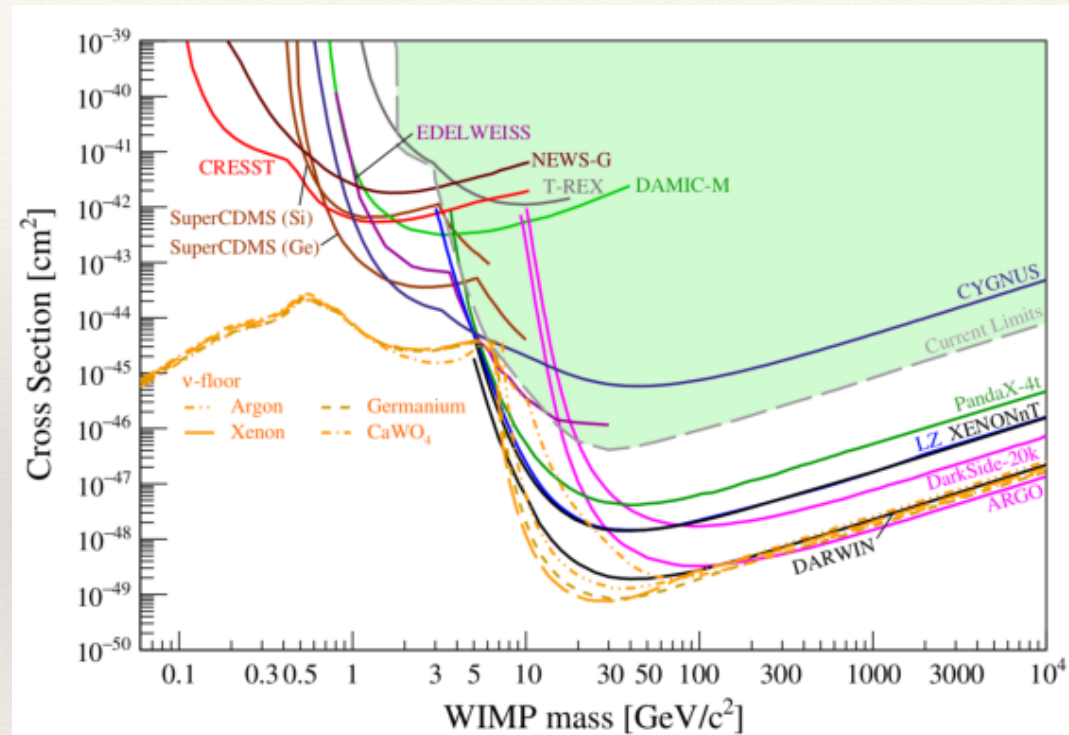
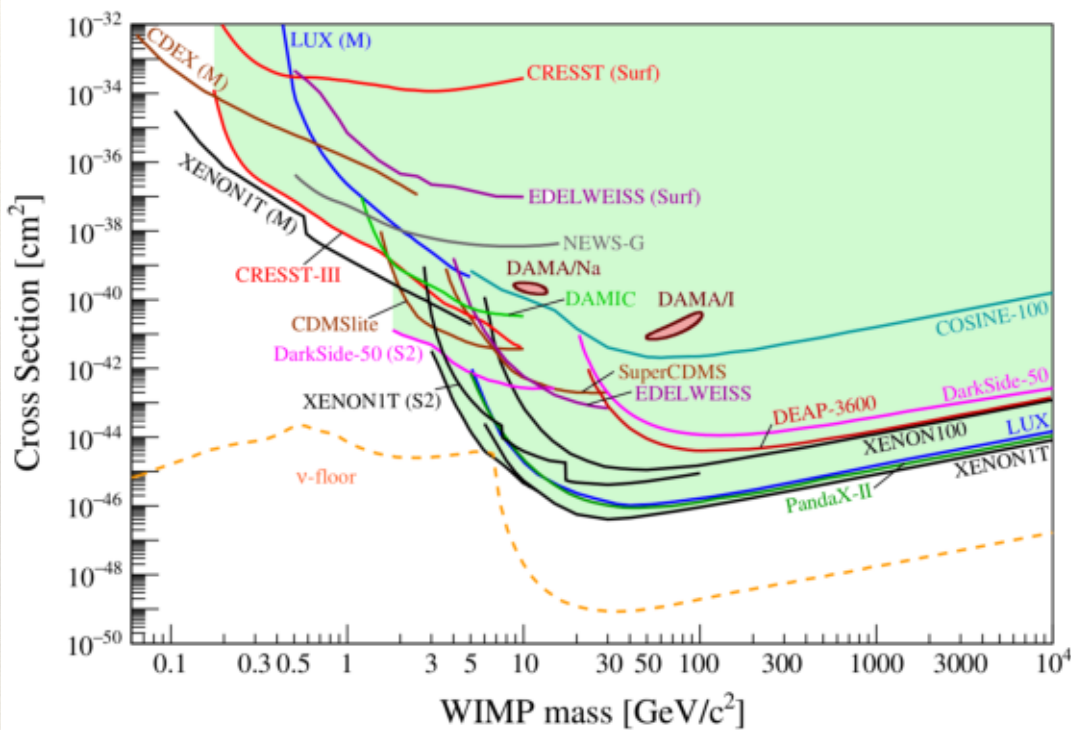


FIG. 5: 90% confidence level upper limit on  $\sigma_{SI}$  from this work (thick black line) with the  $1\sigma$  (green) and  $2\sigma$  (yellow) sensitivity bands. Previous results from LUX [6] and PandaX-II [7] are shown for comparison. The inset shows these limits and corresponding  $\pm 1\sigma$  bands normalized to the median of this work's sensitivity band. The normalized median of the PandaX-II sensitivity band is shown as a dotted line.

# Overview of the direct detection



- ❖ Current status and the future prospects
  - ❖ Going down -> Bigger detectors -> Change to Argon?
  - ❖ Going left -> better energy threshold or new ideas

# Dark Matter detectors

❖ Ton scale



❖ Kilo-ton scale

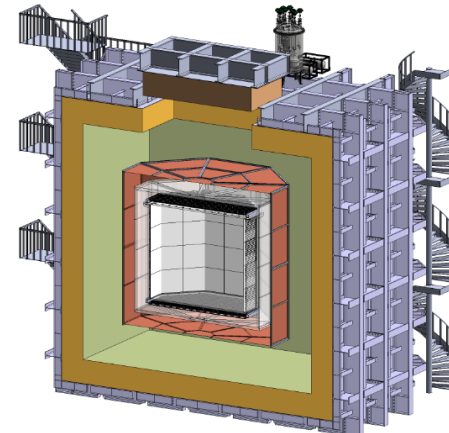


FIG. 4. 3D schematics of the DarkSide-20k experiment. The drawing shows the PPMA TPC filled with UAr, surrounded by the VETO detector made of Gd-loaded PMMA shell sandwiched between two AAr active layers (the inner one, named IAB and the outer one, named OAB in the text), all contained in the ProtoDUNE-like cryostat. The OAB is optically separated by the AAr in contact with the cryostat wall by a membrane, whose characteristics are yet to be defined.

# Annual modulation

- ❖ The Earth is moving around the Sun
- ❖ The Sun is moving in the dark matter halo (which is on average at rest in the Galaxy frame )
- ❖ When the Earth is moving in the same direction with the Sun
  - ❖ Experience a higher averaged dark matter velocity => more event rate!

PHYSICAL REVIEW D

VOLUME 33, NUMBER 12

15 JUNE 1986

## Detecting cold dark-matter candidates

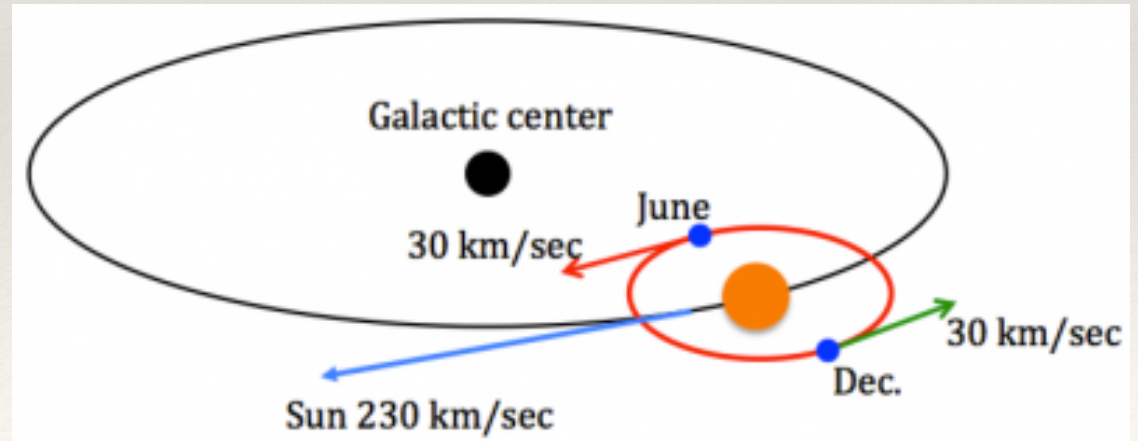
Andrzej K. Drucker

Max-Planck-Institut für Physik und Astrophysik, 8046 Garching, West Germany  
and Department of Astronomy, Harvard-Smithsonian Center for Astrophysics,  
60 Garden Street, Cambridge, Massachusetts 02138

Katherine Freese and David N. Spergel

Department of Astronomy, Harvard-Smithsonian Center for Astrophysics, 60 Garden Street,  
Cambridge, Massachusetts 02138  
(Received 2 August 1985)

We consider the use of superheated superconducting colloids as detectors of weakly interacting galactic-halo candidate particles (e.g., photons, massive neutrinos, and scalar neutrinos). We discuss realistic models for the detector and for the galactic halo. We show that the expected count rate ( $\approx 10^3$  count/day for scalar and massive neutrinos) exceeds the expected background by several orders of magnitude. For photons, we expect  $\approx 1$  count/day, more than 100 times the predicted background rate. We find that if the detector temperature is maintained at 50 mK and using SQUID electronic read out with the system, noise is reduced below  $5 \times 10^{-4}$  flux quanta, particles with mass as low as 2 GeV can be detected. Any particle capable of resolving the solar-neutrino problem by altering energy transport in the Sun can be detected. We show that Earth's motion around the Sun can produce a significant annual modulation in the signal.



# DAMA excess

- ❖ The DAMA experiment has been reporting a positive detection since 2000-ish
- ❖ No good explanations....

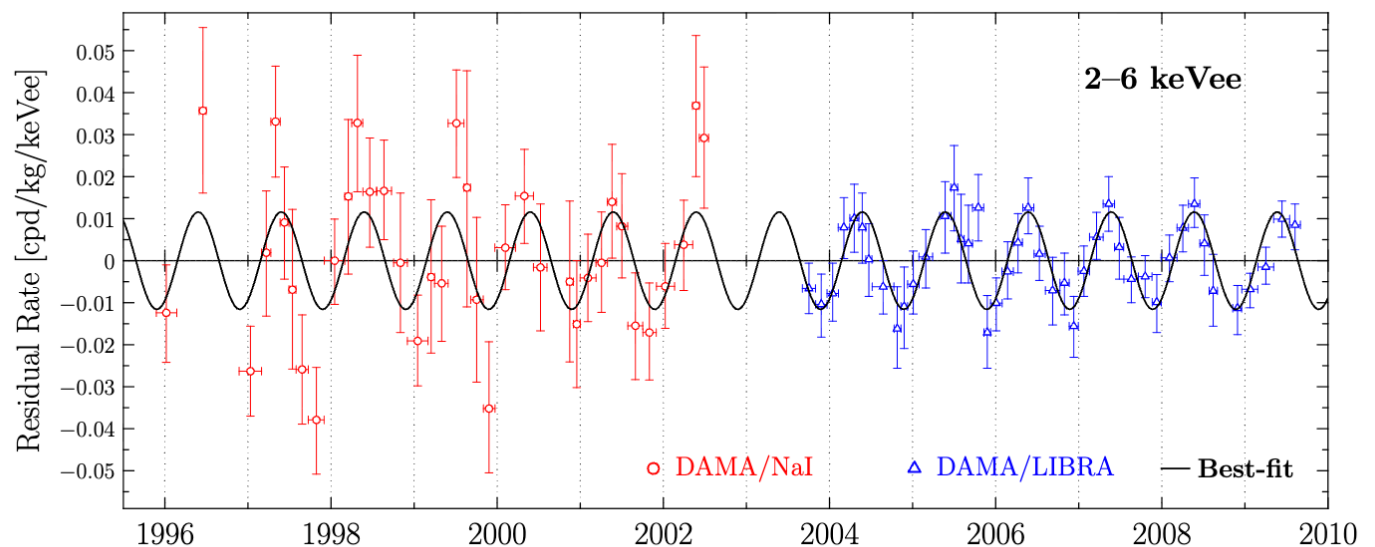
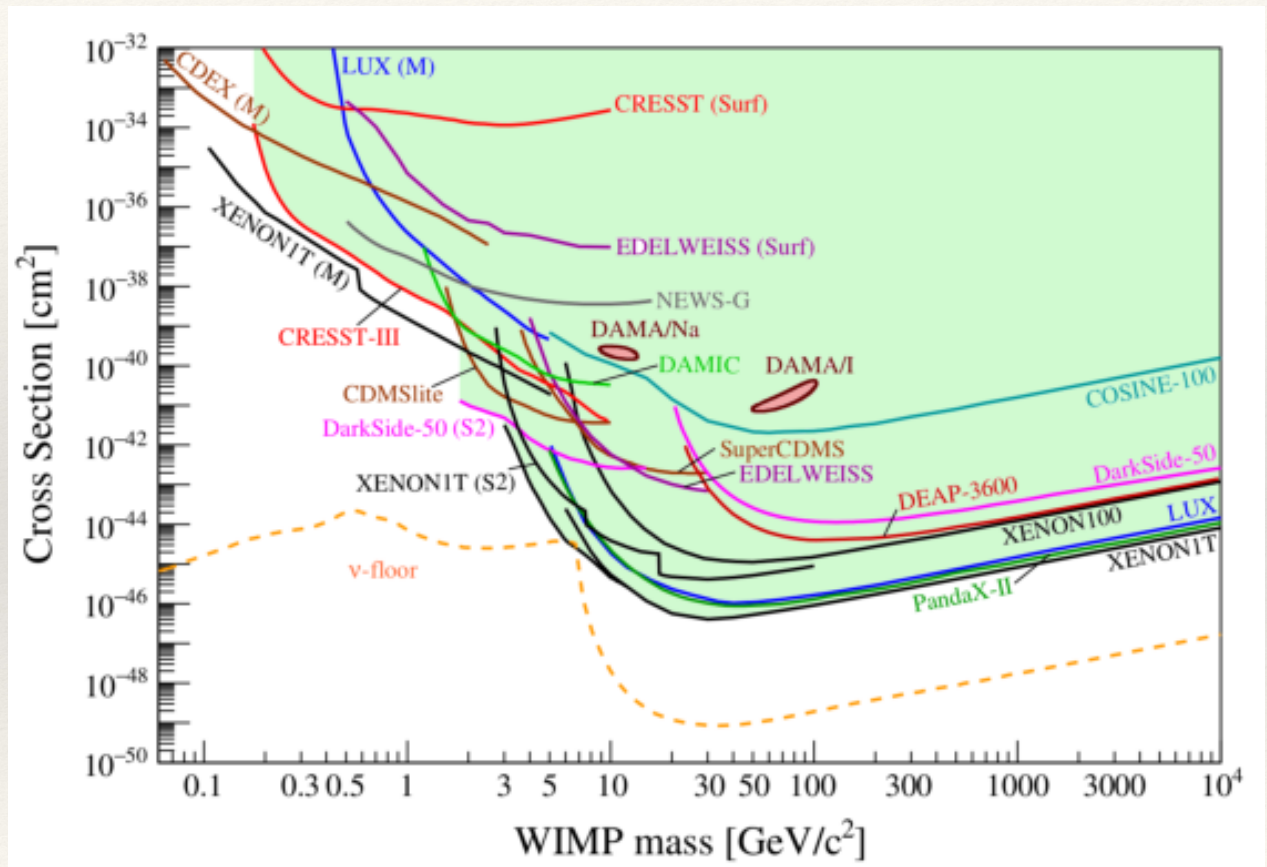


FIG. 5: The residual rate measured by DAMA/NaI (red circles, 0.29 ton-yr exposure over 1995–2002) and DAMA/LIBRA (blue triangles, 0.87 ton-yr exposure over 2003–2010) in the 2–6 keVee energy interval, as a function of time. Data is taken from Refs. [28, 30]. The solid black line is the best fit sinusoidal modulation  $A \cos[\frac{2\pi}{T}(t - t_0)]$  with an amplitude  $A = 0.0116 \pm 0.0013$  cpd/kg/keV, a phase  $t_0 = 0.400 \pm 0.019$  yr (May 26  $\pm$  7 days), and a period  $T = 0.999 \pm 0.002$  yr [30]. The data are consistent with the SHM expected phase of June 1.

# DAMA excess

- ❖ The claim is inconsistent with null detections or all other detectors



# Xenon excess

PHYSICAL REVIEW D **102**, 072004 (2020)

Featured in Physics

## Excess electronic recoil events in XENON1T

E. Aprile,<sup>1</sup> J. Aalbers,<sup>2</sup> F. Agostini,<sup>3</sup> M. Alfonsi,<sup>4</sup> L. Althueser,<sup>5</sup> F. D. Amaro,<sup>6</sup> V. C. Antochi,<sup>2</sup> E. Angelino,<sup>7</sup> J. R. Angevaare,<sup>8</sup> F. Arneodo,<sup>9</sup> D. Barge,<sup>2</sup> L. Baudis,<sup>10</sup> B. Bauermeister,<sup>2</sup> L. Bellagamba,<sup>3</sup> M. L. Benabderahmane,<sup>9</sup> T. Berger,<sup>11</sup> A. Brown,<sup>10</sup> E. Brown,<sup>11</sup> S. Bruenner,<sup>8</sup> G. Bruno,<sup>9</sup> R. Budnik,<sup>12,\*</sup> C. Capelli,<sup>10</sup> J. M. R. Cardoso,<sup>6</sup> D. Cichon,<sup>13</sup> B. Cimmino,<sup>14</sup> M. Clark,<sup>15</sup> D. Coderre,<sup>16</sup> A. P. Colijn,<sup>8,†</sup> J. Conrad,<sup>2</sup> J. P. Cussonneau,<sup>17</sup> M. P. Decowski,<sup>8</sup> A. Depoian,<sup>15</sup> P. Di Gangi,<sup>3</sup> A. Di Giovanni,<sup>9</sup> R. Di Stefano,<sup>14</sup> S. Diglio,<sup>17</sup> A. Elykov,<sup>16</sup> G. Eurin,<sup>13</sup> A. D. Ferella,<sup>18,19</sup> W. Fulgione,<sup>7,19</sup> P. Gaemers,<sup>8</sup> R. Gaior,<sup>20</sup> M. Galloway,<sup>10,‡</sup> F. Gao,<sup>1</sup> L. Grandi,<sup>21</sup> C. Hasterok,<sup>13</sup> C. Hils,<sup>4</sup> K. Hiraide,<sup>22</sup> L. Hoetzsch,<sup>13</sup> J. Howlett,<sup>1</sup> M. Iacobacci,<sup>14</sup> Y. Itow,<sup>23</sup> F. Joerg,<sup>13</sup> N. Kato,<sup>22</sup> S. Kazama,<sup>23,§</sup> M. Kobayashi,<sup>1</sup> G. Koltman,<sup>12</sup> A. Kopec,<sup>15</sup> H. Landsman,<sup>12</sup> R. F. Lang,<sup>15</sup> L. Levinson,<sup>12</sup> Q. Lin,<sup>1</sup> S. Lindemann,<sup>16</sup> M. Lindner,<sup>13</sup> F. Lombardi,<sup>6</sup> J. Long,<sup>21</sup> J. A. M. Lopes,<sup>6,||</sup> E. López Fune,<sup>20</sup> C. Macolino,<sup>24</sup> J. Mahlstedt,<sup>2</sup> A. Mancuso,<sup>3</sup> L. Manenti,<sup>9</sup> A. Manfredini,<sup>10</sup> F. Marignetti,<sup>14</sup> T. Marrodán Undagoitia,<sup>13</sup> K. Martens,<sup>22</sup> J. Masbou,<sup>17</sup> D. Masson,<sup>16</sup> S. Mastroianni,<sup>14</sup> M. Messina,<sup>19</sup> K. Miuchi,<sup>25</sup> K. Mizukoshi,<sup>25</sup> A. Molinaro,<sup>19</sup> K. Morå,<sup>1,2</sup> S. Moriyama,<sup>22</sup> Y. Mosbacher,<sup>12</sup> M. Murra,<sup>5</sup> J. Naganoma,<sup>19</sup> K. Ni,<sup>26</sup> U. Oberlack,<sup>4</sup> K. Odgers,<sup>11</sup> J. Palacio,<sup>13,17</sup> B. Pelssers,<sup>2</sup> R. Peres,<sup>10</sup> J. Pienaar,<sup>21</sup> V. Pizzella,<sup>13</sup> G. Plante,<sup>1</sup> J. Qin,<sup>15</sup> H. Qiu,<sup>12</sup> D. Ramírez García,<sup>16</sup> S. Reichard,<sup>10</sup> A. Rocchetti,<sup>16</sup> N. Rupp,<sup>13</sup> J. M. F. dos Santos,<sup>6</sup> G. Sartorelli,<sup>3</sup> N. Šarčević,<sup>16</sup> M. Scheibelhut,<sup>4</sup> J. Schreiner,<sup>13</sup> D. Schulte,<sup>5</sup> M. Schumann,<sup>16</sup> L. Scotto Lavina,<sup>20</sup> M. Selvi,<sup>3</sup> F. Semeria,<sup>3</sup> P. Shagin,<sup>27</sup> E. Shockley,<sup>21,¶</sup> M. Silva,<sup>6</sup> H. Simgen,<sup>13</sup> A. Takeda,<sup>22</sup> C. Therreau,<sup>17</sup> D. Thers,<sup>17</sup> F. Toschi,<sup>16</sup> G. Trinchero,<sup>7</sup> C. Tunnell,<sup>27</sup> M. Vargas,<sup>5</sup> G. Volta,<sup>10</sup> H. Wang,<sup>28</sup> Y. Wei,<sup>26</sup> C. Weinheimer,<sup>5</sup> M. Weiss,<sup>12</sup> D. Wenz,<sup>4</sup> C. Wittweg,<sup>5</sup> Z. Xu,<sup>1</sup> M. Yamashita,<sup>23,22</sup> J. Ye,<sup>10,\*\*\*</sup> G. Zavattini,<sup>3,††</sup> Y. Zhang,<sup>1</sup> T. Zhu,<sup>1</sup> and J. P. Zopounidis,<sup>20</sup>

(XENON Collaboration)<sup>‡‡</sup>

X. Mougeot<sup>29</sup>

# Xenon excess

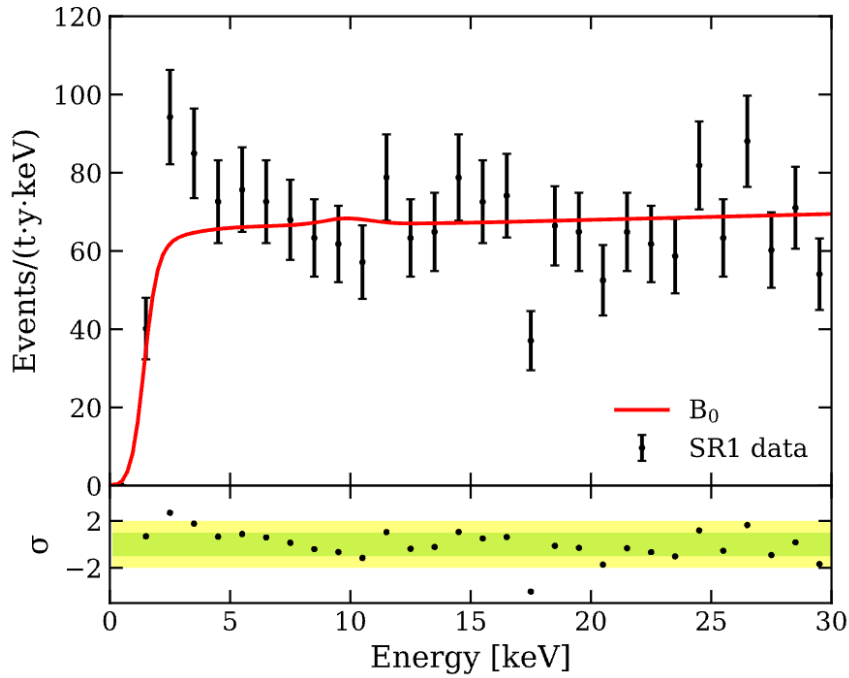
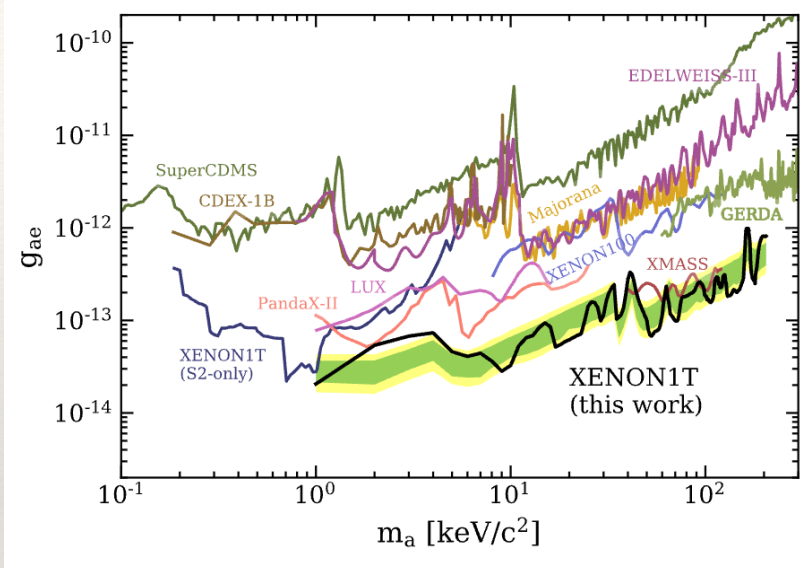


FIG. 4. A zoomed-in and rebinned version of Fig. 3 (top), where the data display an excess over the background model  $B_0$ . In the following sections, this excess is interpreted under solar axion, neutrino magnetic moment, and tritium hypotheses.



❖ Solar Axions?

## Excess electronic recoil events in XENON1T

XENON Collaboration • E. Aprile (Columbia U.) [Show All\(139\)](#)

Jun 17, 2020

26 pages

Published in: *Phys.Rev.D* 102 (2020) 7, 072004

Published: Oct 13, 2020

e-Print: [2006.09721](#) [hep-ex]

DOI: [10.1103/PhysRevD.102.072004](#)

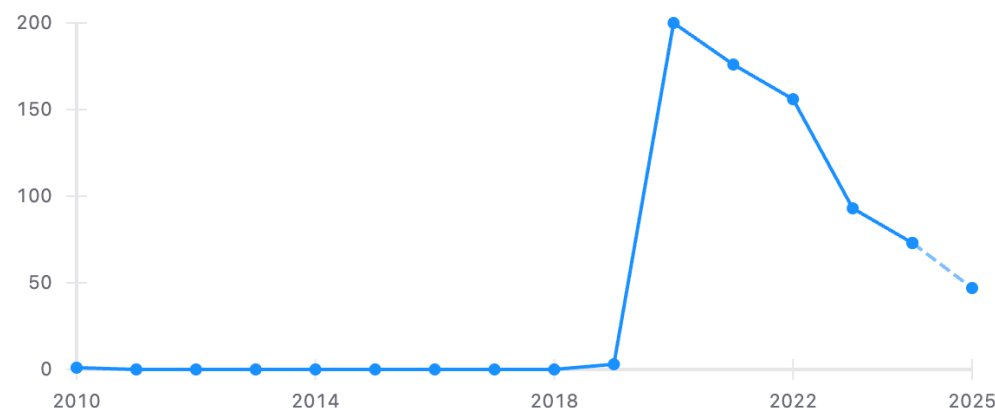
PDG: Limit on Invisible  $A^0$  (Axion) Electron Coupling [Show All\(5\)](#)

Experiments: XENON1T

View in: [HAL Science Ouverte](#), [ADS Abstract Service](#)

[pdf](#) [links](#) [cite](#) [claim](#) [reference search](#) [749 citations](#)

### Citations per year



arXiv > hep-ex > arXiv:2006.13278

Search..

Help | A

## High Energy Physics – Experiment

[Submitted on 23 Jun 2020 ([v1](#)), last revised 25 Jun 2020 (this version, [v2](#))]

# XENON1T observes tritium

Alan E. Robinson

XENON1T recently reported an excess of low-energy electron recoil events that may be attributable to either new physics or to the radioactive decay of tritium. It is likely that hydrogen is not be effectively removed by the hot zirconium getters deployed in the detector. Cosmogenic activation of the xenon underground is found to be insufficient to describe the observed excess, although gases diffusing out of detector materials from cosmogenic activation on surface may contribute. Changes in the operation of gas purification systems for XENON1T and other liquid noble gas detectors could both confirm the tritium hypothesis and remove it from the detector.



# Neutrino Floor

- ❖ As direct detection gets better
- ❖ They can eventually see even neutrino neutral current interactions
- ❖  $\nu + N \rightarrow \nu + N$
- ❖ Then it becomes difficult to distinguish dark matter and neutrino events

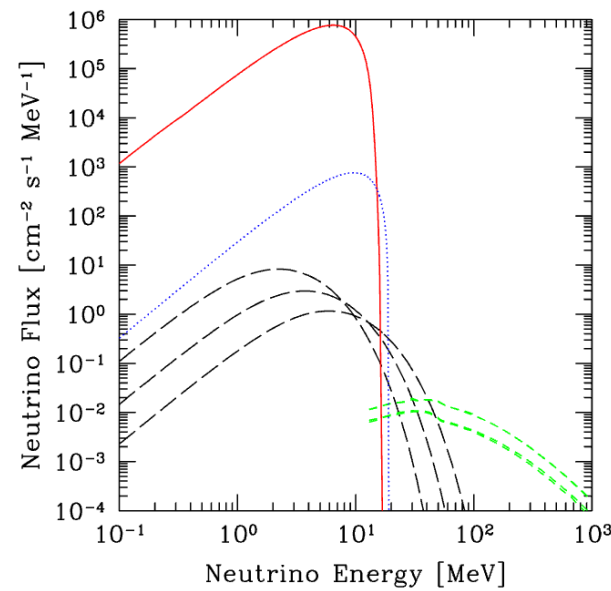
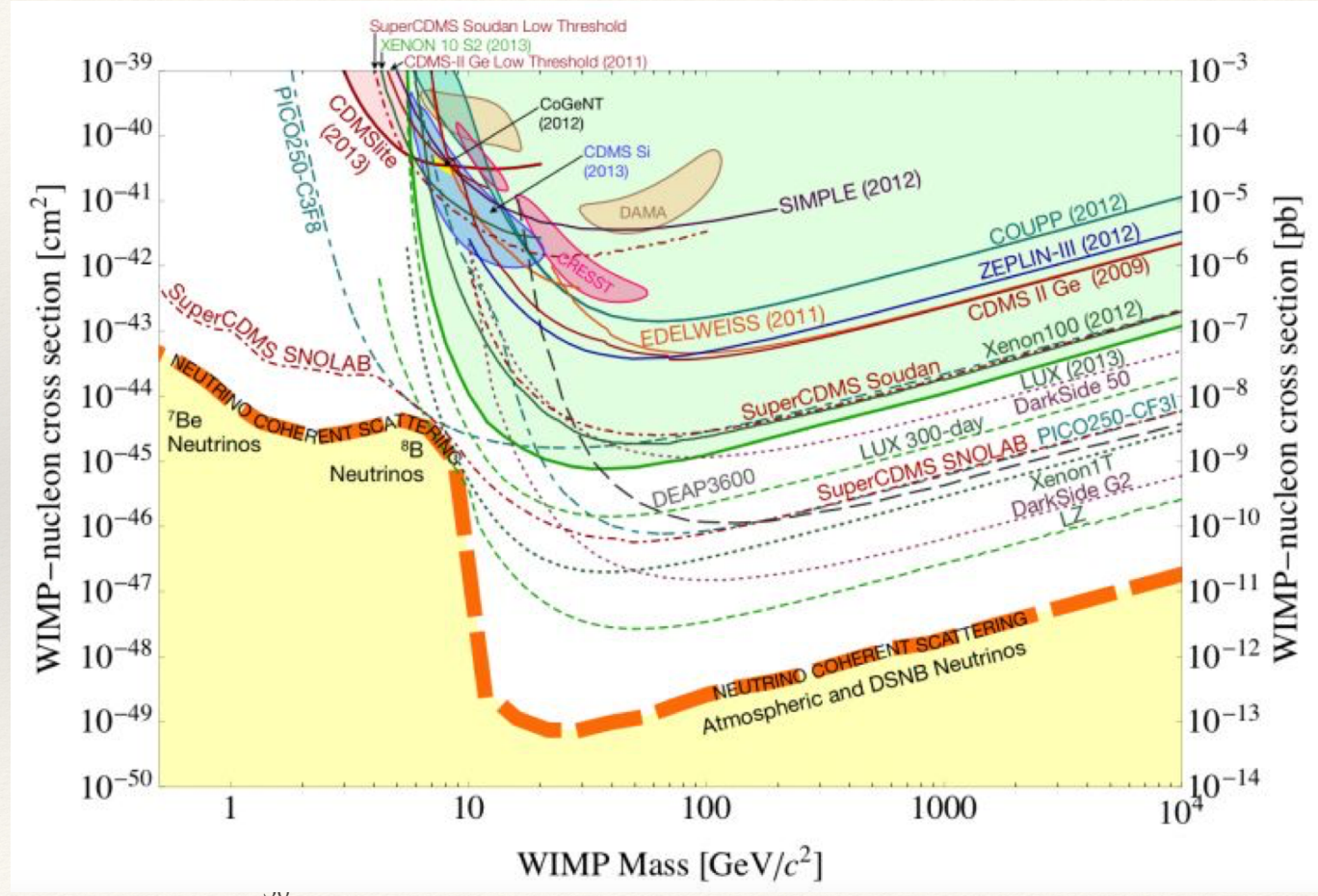


**Figure 1.** Neutrino fluxes for astrophysical sources that constitute the dominant backgrounds to WIMP recoil signals. From top to bottom on the left, the fluxes are solar  ${}^8\text{B}$  (solid, red) and  $hep$  (dotted, blue), DSNB (long-dash, black) with temperatures of 3, 5 and 8 MeV (corresponding to  $\nu_e$ ,  $\bar{\nu}_e$  and  $\nu_x$ , respectively, where  $\nu_x$  symbolizes muon and tau neutrinos and the respective antiparticles). The short-dashed (green) curves at the highest energies are the atmospheric neutrino fluxes, plotted down to the lowest energy in the calculation of [15]. From bottom to top on the right, the fluxes are for  $\nu_e$ ,  $\bar{\nu}_e$ , then  $\nu_\mu$ ,  $\bar{\nu}_\mu$ .

# Neutrino Floor

- ❖ As direct detection gets better
- ❖ They can eventually see even neutrino neutral current interactions
- ❖  $\nu + N \rightarrow \nu + N$
- ❖ Then it becomes difficult to distinguish dark matter and neutrino events



## First Indication of Solar ${}^8\text{B}$ Neutrinos via Coherent Elastic Neutrino-Nucleus Scattering with XENONnT

E. Aprile<sup>1</sup>, J. Aalbers<sup>2</sup>, K. Abe<sup>3</sup>, S. Ahmed Maouloud<sup>4</sup>, L. Althueser<sup>5</sup>, B. Andrieu<sup>6</sup>, E. Angelino<sup>6,7</sup>, D. Antón Martin<sup>8</sup>, F. Arneodo<sup>9</sup>, L. Baudis<sup>10</sup>, M. Bazyk<sup>11</sup>, L. Bellagamba<sup>12</sup>, R. Biondi<sup>13</sup>, A. Bismark<sup>10</sup>, K. Boese<sup>13</sup>, A. Brown<sup>14</sup>, G. Bruno<sup>11</sup>, R. Budnik<sup>15</sup>, C. Cai,<sup>16</sup> C. Capelli<sup>10</sup>, J. M. R. Cardoso<sup>17</sup>, A. P. Cimental Chávez<sup>10</sup>, A. P. Colijn<sup>18</sup>, J. Conrad<sup>19</sup>, J. J. Cuenca-García<sup>10</sup>, V. D'Andrea<sup>7,\*</sup>, L. C. Daniel Garcia<sup>10</sup>, M. P. Decowski<sup>18</sup>, A. Deisting<sup>20</sup>, C. Di Donato<sup>21,7</sup>, P. Di Gangi<sup>12</sup>, S. Diglio<sup>11</sup>, K. Eitel<sup>22</sup>, A. Elykov<sup>22</sup>, A. D. Ferella<sup>21,7</sup>, C. Ferrari<sup>10</sup>, H. Fischer<sup>14</sup>, T. Flehmke<sup>19</sup>, M. Flierman<sup>18</sup>, W. Fulgione<sup>10</sup>, C. Fuselli<sup>18</sup>, P. Gaemers<sup>18</sup>, R. Gaior<sup>4</sup>, M. Galloway<sup>10</sup>, F. Gao<sup>16</sup>, S. Ghosh<sup>23</sup>, R. Giacomobono<sup>24</sup>, R. Glade-Beucke<sup>14</sup>, L. Grandi<sup>8</sup>, J. Grigat<sup>14</sup>, H. Guan<sup>23</sup>, M. Guida<sup>13</sup>, P. Gyorgy<sup>20</sup>, R. Hammann<sup>13</sup>, A. Higuera<sup>25</sup>, C. Hils<sup>20</sup>, L. Hoetzsch<sup>13</sup>, N. F. Hood<sup>26</sup>, M. Iacovacci<sup>24</sup>, Y. Itow<sup>27</sup>, J. Jakob<sup>5</sup>, F. Joerg<sup>13,10</sup>, Y. Kaminaga<sup>10</sup>, M. Kara<sup>22</sup>, P. Kavrigin<sup>15</sup>, S. Kazama<sup>27</sup>, M. Kobayashi<sup>27</sup>, D. Koke<sup>5</sup>, A. Kopec<sup>26,†</sup>, F. Kuger<sup>14</sup>, H. Landsman<sup>15</sup>, R. F. Lang<sup>23</sup>, L. Levinson<sup>15</sup>, I. Li<sup>25</sup>, S. Li<sup>28</sup>, S. Liang<sup>13</sup>, Y.-T. Lin<sup>13</sup>, S. Lindemann<sup>14</sup>, M. Lindner<sup>13</sup>, K. Liu<sup>16,‡</sup>, M. Liu,<sup>1,16</sup> J. Loizeau<sup>11</sup>, F. Lombardi<sup>20</sup>, J. Long<sup>8</sup>, J. A. M. Lopes<sup>17,§</sup>, T. Luce<sup>14</sup>, Y. Ma<sup>26</sup>, C. Macolino<sup>21,7</sup>, J. Mahlstedt<sup>19</sup>, A. Mancuso<sup>12</sup>, L. Manenti<sup>9</sup>, F. Marignetti<sup>24</sup>, T. Marrodán Undagoitia<sup>13</sup>, K. Martens<sup>3</sup>, J. Masbou<sup>11</sup>, E. Masson<sup>4</sup>, S. Mastroianni<sup>24</sup>, A. Melchiorre<sup>21,7</sup>, J. Merz,<sup>20</sup> M. Messina<sup>10</sup>, A. Michael,<sup>5</sup>, K. Miuchi<sup>29</sup>, A. Molinario<sup>6</sup>, S. Moriyama<sup>3</sup>, K. Morå<sup>1</sup>, Y. Mosbacher,<sup>15</sup> M. Murra<sup>1</sup>, J. Müller<sup>14</sup>, K. Ni<sup>26</sup>, U. Oberlack<sup>20</sup>, B. Paetsch<sup>15</sup>, Y. Pan<sup>4</sup>, Q. Pellegrini<sup>4</sup>, R. Peres<sup>10</sup>, C. Peters,<sup>25</sup> J. Pienaar<sup>8,15</sup>, M. Pierre<sup>18</sup>, G. Plante<sup>1</sup>, T. R. Pollmann<sup>18</sup>, L. Principe<sup>11</sup>, J. Qi<sup>26</sup>, J. Qin<sup>25</sup>, D. Ramírez García<sup>10</sup>, M. Rajado<sup>10</sup>, R. Singh<sup>23</sup>, L. Sanchez<sup>25</sup>, J. M. F. dos Santos<sup>17</sup>, I. Sarnoff<sup>9</sup>, G. Sartorelli<sup>12</sup>, J. Schreiner,<sup>13</sup> P. Schulze<sup>5</sup>, H. Schulze Eißing<sup>5</sup>, M. Schumann<sup>14</sup>, L. Scotto Lavina<sup>4</sup>, M. Selvi<sup>12</sup>, F. Semeria<sup>12</sup>, P. Shagin<sup>20</sup>, S. Shi<sup>1</sup>, J. Shi,<sup>16</sup> M. Silva<sup>17</sup>, H. Simgen<sup>13</sup>, A. Takeda<sup>3</sup>, P.-L. Tan<sup>19</sup>, D. Thers<sup>11</sup>, F. Toschi<sup>22</sup>, G. Trinchero<sup>6</sup>, C. D. Tunnell<sup>25</sup>, F. Tönnies<sup>14</sup>, K. Valerius<sup>22</sup>, S. Vecchi<sup>30</sup>, S. Vetter<sup>22</sup>, F. I. Villazon Solar,<sup>20</sup> G. Volta<sup>13</sup>, C. Weinheimer<sup>5</sup>, M. Weiss<sup>15</sup>, D. Wenz<sup>5</sup>, C. Wittweg<sup>10</sup>, V. H. S. Wu<sup>22</sup>, Y. Xing<sup>11</sup>, D. Xu<sup>1,||</sup>, Z. Xu<sup>1</sup>, M. Yamashita<sup>3</sup>, L. Yang<sup>26</sup>, J. Ye<sup>31,¶</sup>, L. Yuan<sup>8</sup>, G. Zavattini<sup>30</sup> and M. Zhong<sup>26</sup>

(XENON Collaboration)

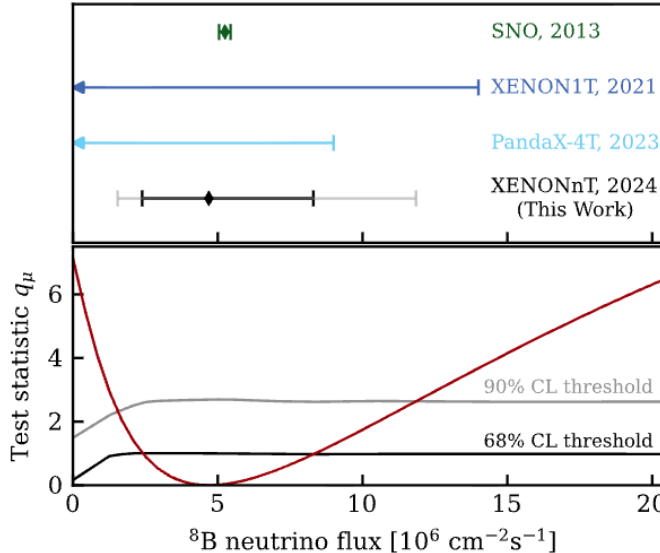
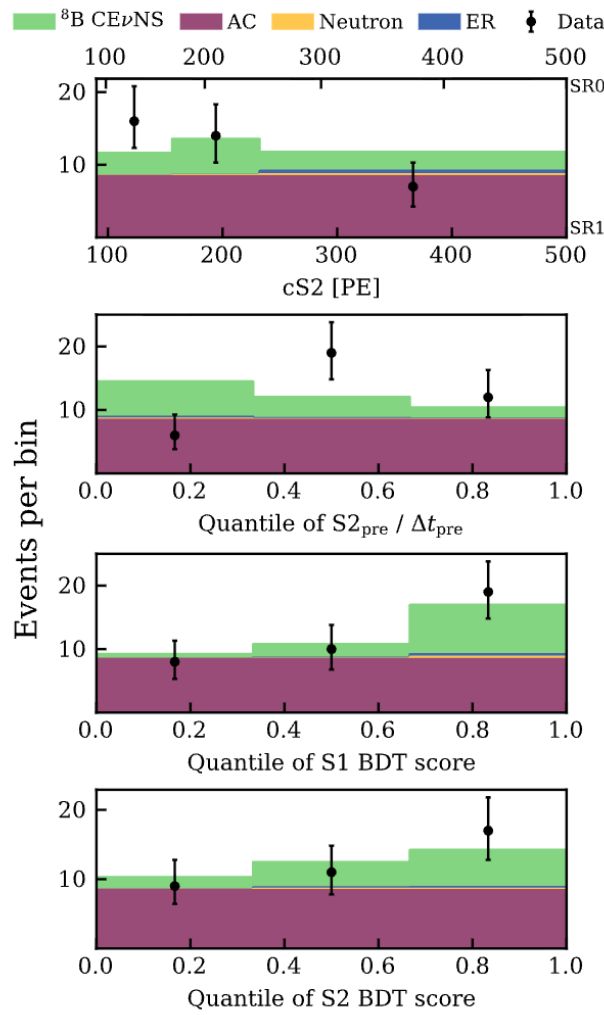


FIG. 3. Constraints on solar  ${}^8\text{B}$  neutrino flux. Top: the 68% (90%) measurement of solar  ${}^8\text{B}$  neutrino flux from this work is shown in black (gray). The 68% CL measurement from SNO [23] and 90% CL upper limits from XENON1T [7] and PandaX-4T [8] are also shown. Bottom: the solid red line shows the profile likelihood ratio test statistics  $q_\mu$  as a function of solar  ${}^8\text{B}$  neutrino flux. The constraints are derived with Feldman-Cousins construction at 68% (90%) CL, indicated by the black (gray) curve.

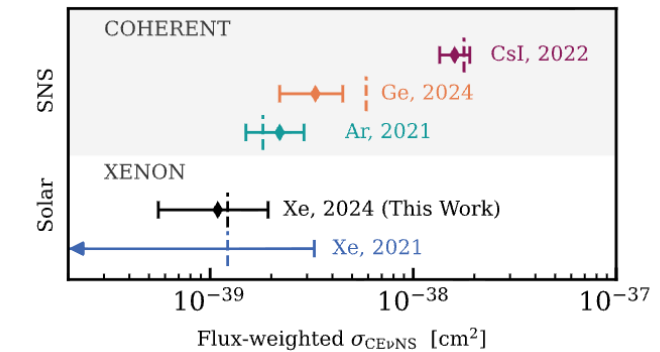
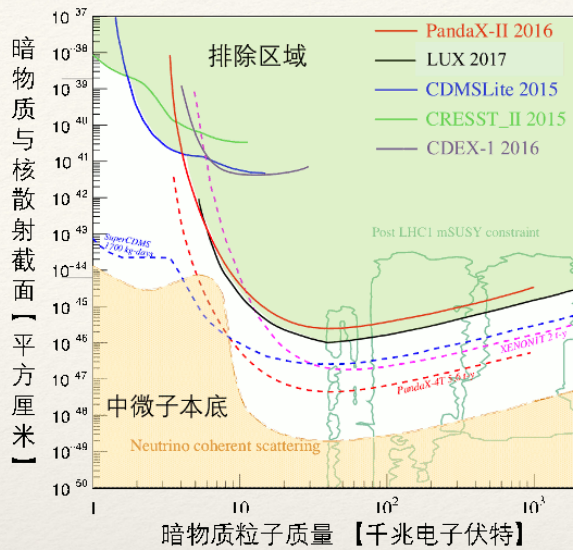


FIG. 4. Measurements of the flux-weighted  $\text{CE}\nu\text{NS}$  cross section  $\sigma_{\text{CE}\nu\text{NS}}$ . The measurement using Xe nuclei solar  ${}^8\text{B}$  neutrinos from this work is shown in black. The 90% CL upper limit from XENON1T [7] is shown in blue. The measurements with neutrinos from the SNS by the COHERENT Collaboration using CsI [44] (red), Ar [5] (green), and Ge [45] (orange) nuclei are also shown. For comparison, the SM predictions are shown by vertical dashed lines.

# The PandaX project in CJPL

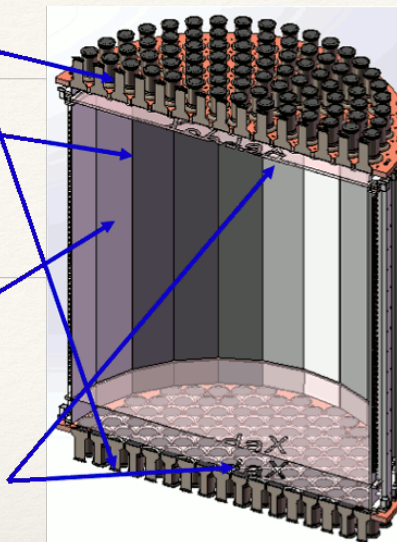


**光电管:** 收集探测器内的S1和S2光

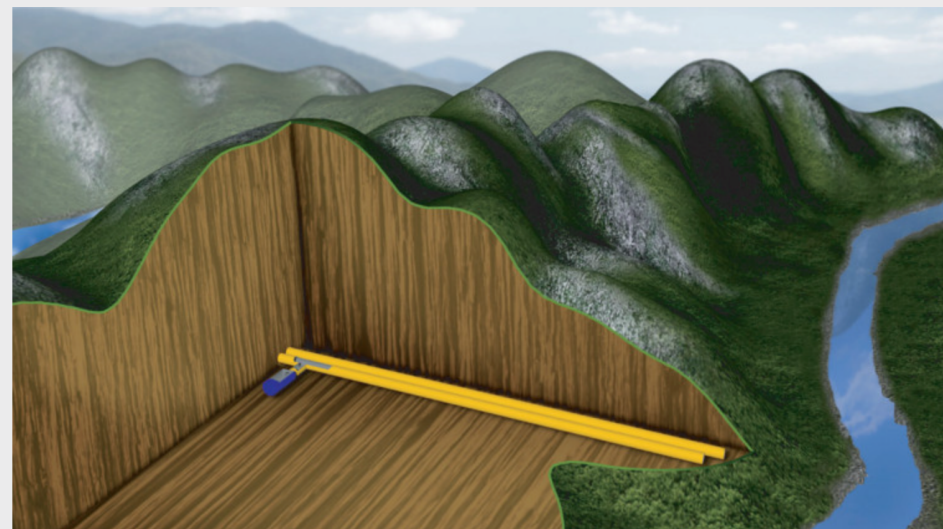
**PTFE壁:** 反射内部的光, 提高光收集效率

**液氙探测材料:** 液状氙在探测器中既是靶子也是探测介质

**高压漂移电场:** 暗物质或放射性事件产生的电子可以通过漂移电场进入气体产生发光

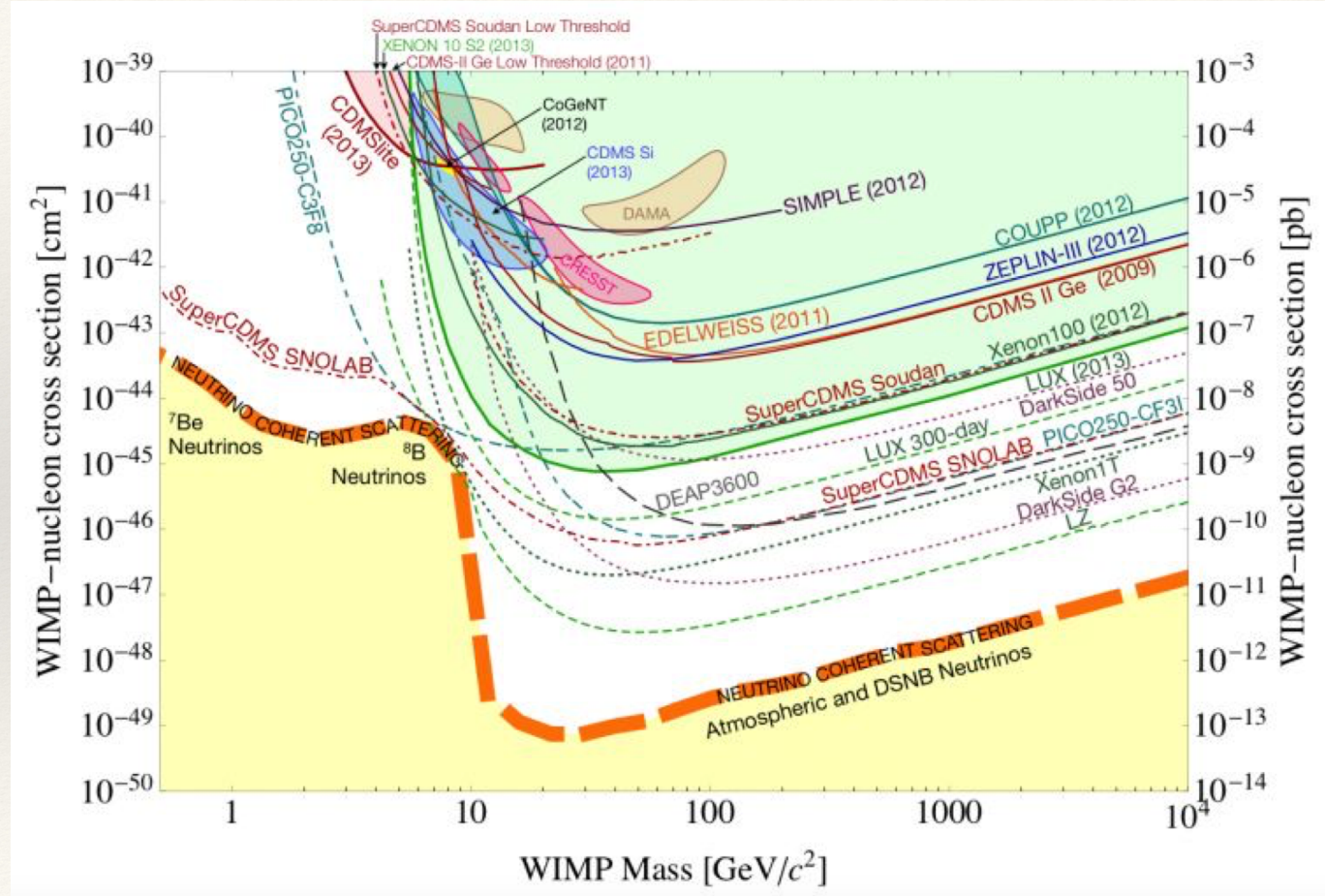


Located in the middle of a 18-km tunnel under 2400 meters of rock overburden, in the Sichuan province of south-west China. As one of the deepest underground labs in the world, the CJPL has an extremely low flux of muon rate of less than  $20/m^2/100$  day, which is about two orders of magnitude lower than the flux at the Gran Sasso underground laboratory (LNGS) in Italy. The low muon rate and the resulting background makes the lab ideal for a sensitive dark matter detection.



# Neutrino Floor

- ❖ As direct detection gets better
- ❖ They can eventually see even neutrino neutral current interactions
- ❖  $\nu + N \rightarrow \nu + N$
- ❖ Then it becomes difficult to distinguish dark matter and neutrino events



# Complementarity

## Complementarity of Dark Matter Searches in the pMSSM

M. Cahill-Rowley<sup>1</sup>, R. Cotta<sup>2</sup>, A. Drlica-Wagner<sup>3</sup>, S. Funk<sup>1</sup>, J.L. Hewett<sup>4</sup>,  
A. Ismail<sup>4,5</sup>, T.G. Rizzo<sup>1</sup>, and M. Wood<sup>1</sup>

<sup>1</sup>SLAC National Accelerator Laboratory, Menlo Park, CA, USA\*

<sup>2</sup>University of California, Irvine, CA, USA†

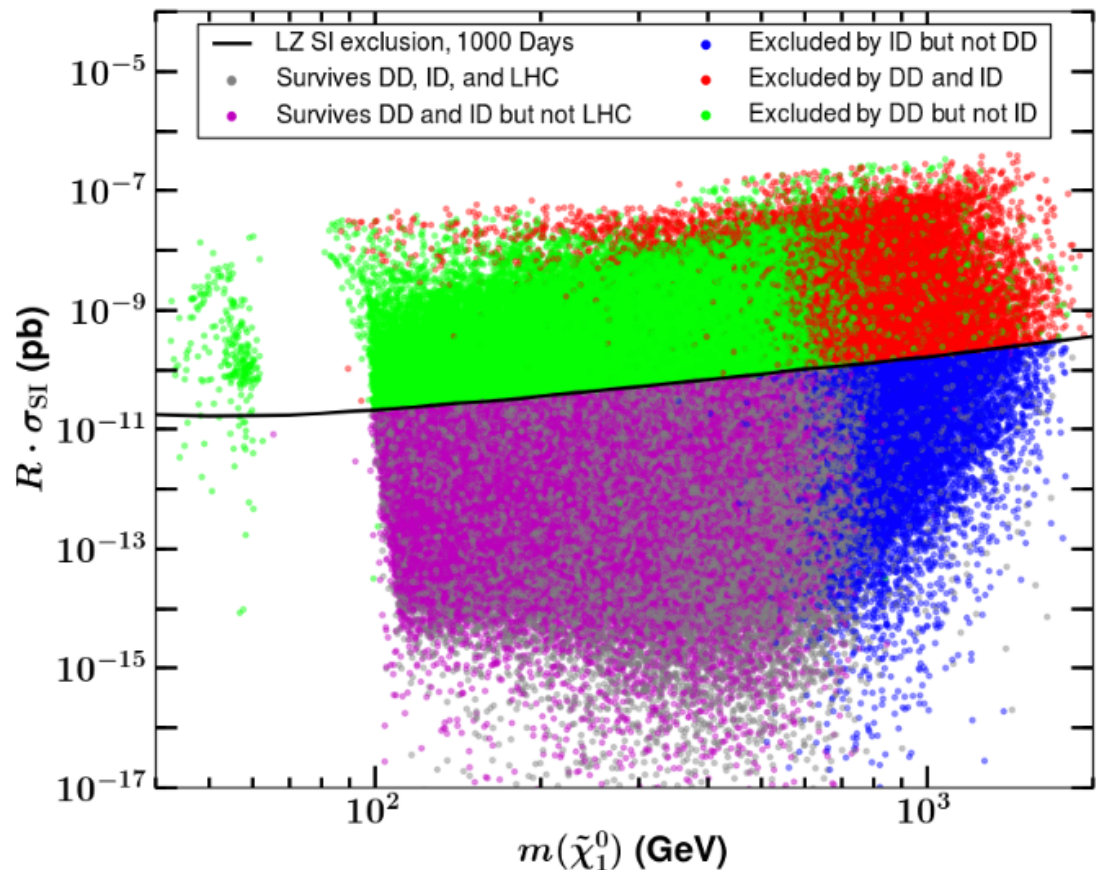
<sup>3</sup>Fermi National Accelerator Laboratory, Batavia, IL, USA‡

<sup>4</sup>Argonne National Laboratory, Argonne, IL, USA§

<sup>5</sup>University of Illinois, Chicago, IL, USA

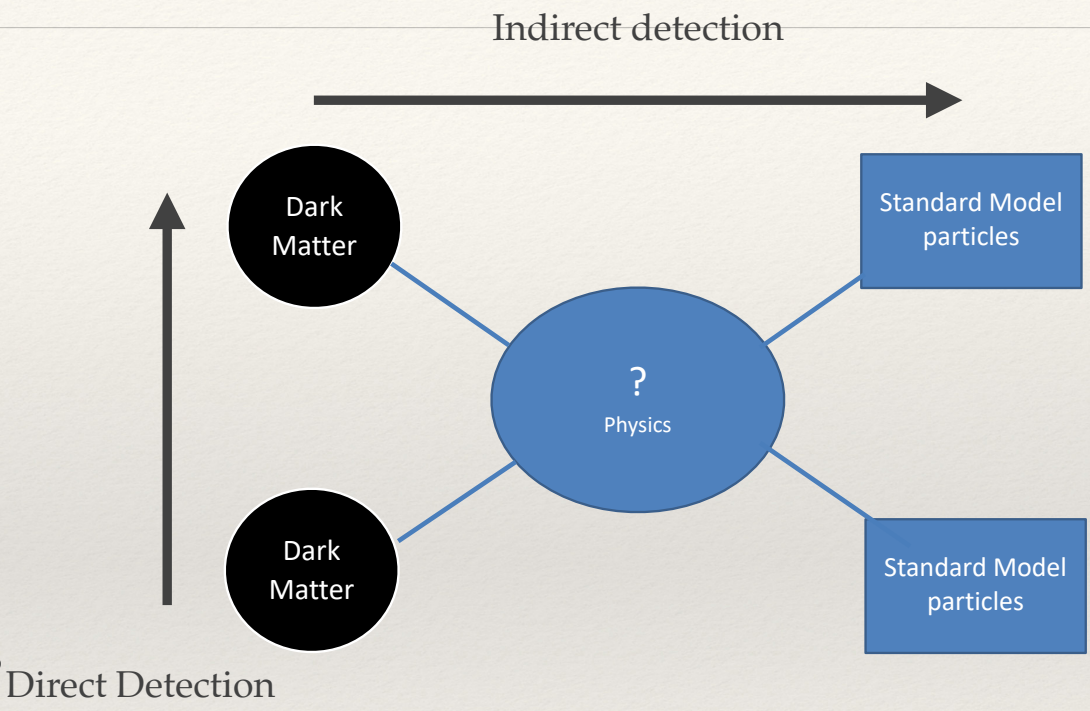
### Abstract

As is well known, the search for and eventual identification of dark matter in supersymmetry requires a simultaneous, multi-pronged approach with important roles played by the LHC as well as both direct and indirect dark matter detection experiments. We examine the capabilities of these approaches in the 19-parameter p(henomenological)MSSM which provides a general framework for complementarity studies of neutralino dark matter. We summarize the sensitivity of dark matter searches at the 7, 8 (and eventually 14) TeV LHC, combined with those by *Fermi*, CTA, Ice-Cube/DeepCore, COUPP, LZ and XENON. The strengths and weaknesses of each of these techniques are examined and contrasted and their interdependent roles in covering the model parameter space are discussed in detail. We find that these approaches explore orthogonal territory and that advances in each are necessary to cover the Supersymmetric WIMP parameter space. We also find that different experiments have widely varying sensitivities to the various dark matter annihilation mechanisms, some of which would be completely excluded by null results from these experiments.

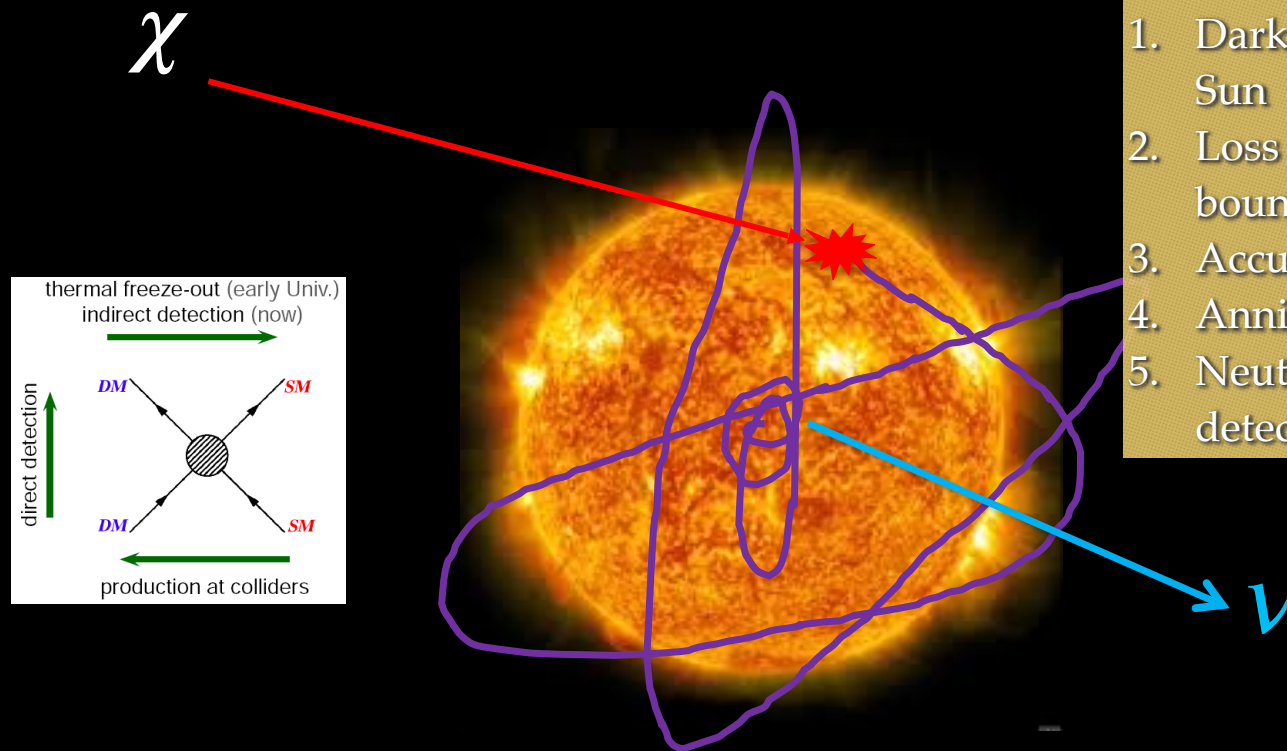


# Search for dark matter from the Sun

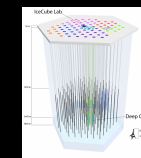
- ❖ As we discussed in the indirect detection chapter
- ❖ Neutrino channels are difficult to probe
- ❖ But there is another way
  
- ❖ If dark matter is WIMP
  - ❖ It should have some DM-nucleon cross section AND annihilation cross section



# Sun – Dark Matter detector



1. Dark Matter first scatter with the Sun
2. Loss energy and be gravitationally bound / captured
3. Accumulate in the centre
4. Annihilate
5. Neutrinos escape, and could be detected!



# Search for dark matter from the Sun

- ❖ The dark matter capture process is described by

$$\frac{dN}{dt} = C - AN^2$$

- ❖  $N$  is the amount of dark matter in the Sun

- ❖  $C$  is the capture term, which does not depends on  $N$

- ❖  $AN^2$  is the annihilation rate (for dark matter destruction),  $\propto N^2$ ,  $= 2 \times \frac{1}{2}AN^2$  because each reaction takes away 2 dark matter

- ❖ The system achieves equilibrium eventually.

$$dN/dt \rightarrow 0, N_0 = \sqrt{\frac{C}{A}}$$

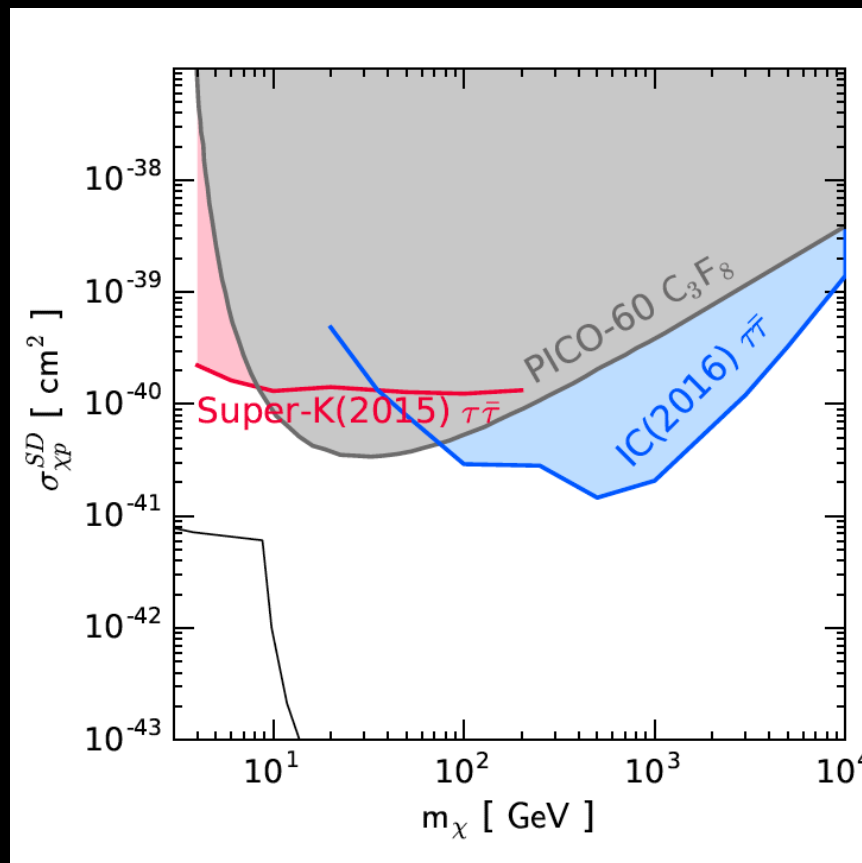
$$\text{The annihilation rate (for signal computation)} = \frac{1}{2}AN_0^2 = \frac{1}{2}C$$

- ❖ Solar dark matter search only tests the Capture process, and thus only the dark matter nucleon cross section

- ❖ The annihilation part, and its channel (only neutrino is observable), needs to be assumed to have certain value that affects the equilibrium process

# Solar WIMP Search

- Best limit on SD cross sections
  - Hard Channels
- Both scattering and Annihilation!
- 



# Cosmic Ray Boosted dark matter search

- ❖ If dark matter direct detection is limited by Speed, is it possible to speed dark matter up?
- ❖ Cosmic rays can interact with dark matter (with the same DM-nucleon cross section)
- ❖ Boost them to relativistic speed!
- ❖ Overcome the detection detector threshold
- ❖ And may be able to use neutrino detectors!

Novel direct detection constraints on light dark matter

Torsten Bringmann<sup>1</sup> and Maxim Pospelov<sup>2,3</sup>

<sup>1</sup>*Department of Physics, University of Oslo, Box 1048, N-0371 Oslo, Norway*

<sup>2</sup>*Perimeter Institute for Theoretical Physics, Waterloo, ON N2J 2W9, Canada*

<sup>3</sup>*Department of Physics and Astronomy, University of Victoria, Victoria, BC V8P 5C2, Canada*

(Dated: June 2018)

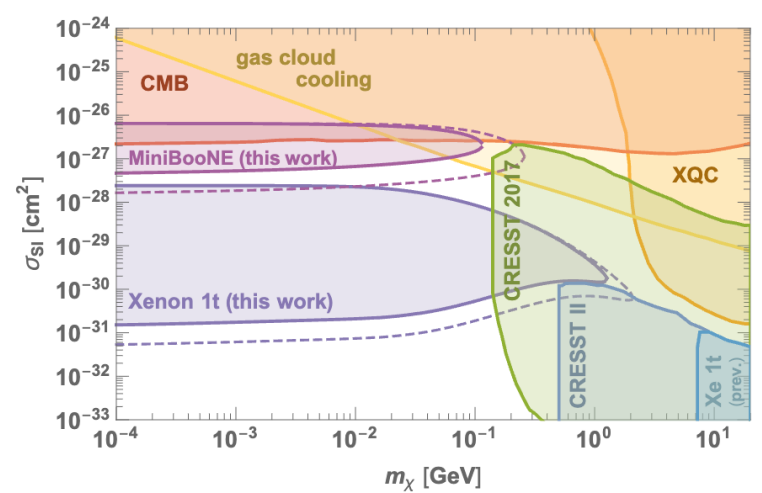
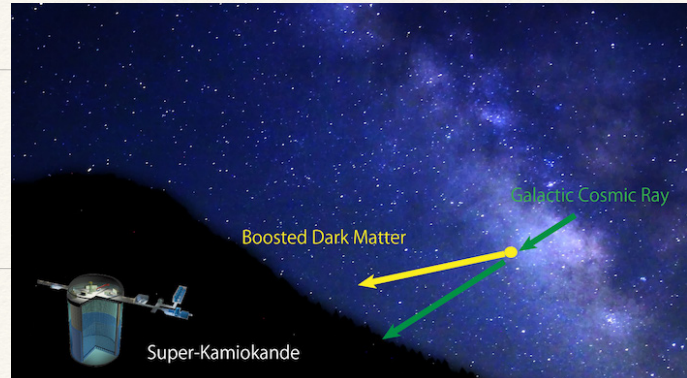


FIG. 2. Constraints on spin-independent DM-nucleon scattering imposed by the XENON-1T and MiniBooNE experiments. Solid (dashed) lines assume a CR density that equals, on average, the local value out to a distance of 1 kpc (10 kpc). We compare our limits to those deriving from CMB observations [40], gas cloud cooling [38], the X-ray Quantum Calorimeter experiment (XQC) [39], and a selection of direct detection experiments [43–45] after taking into account the absorption of DM in soil and atmosphere [33].